Karlsruhe Institute of Technology

wave phenomena
analysis and numerics

Leapfrog Crank–Nicolson decoupling of wave-heat-type problems

Benjamin Dörich, Julian Dörner

CRC Preprint 2026/9, March 2026

KARLSRUHE INSTITUTE OF TECHNOLOGY

CRC 1173

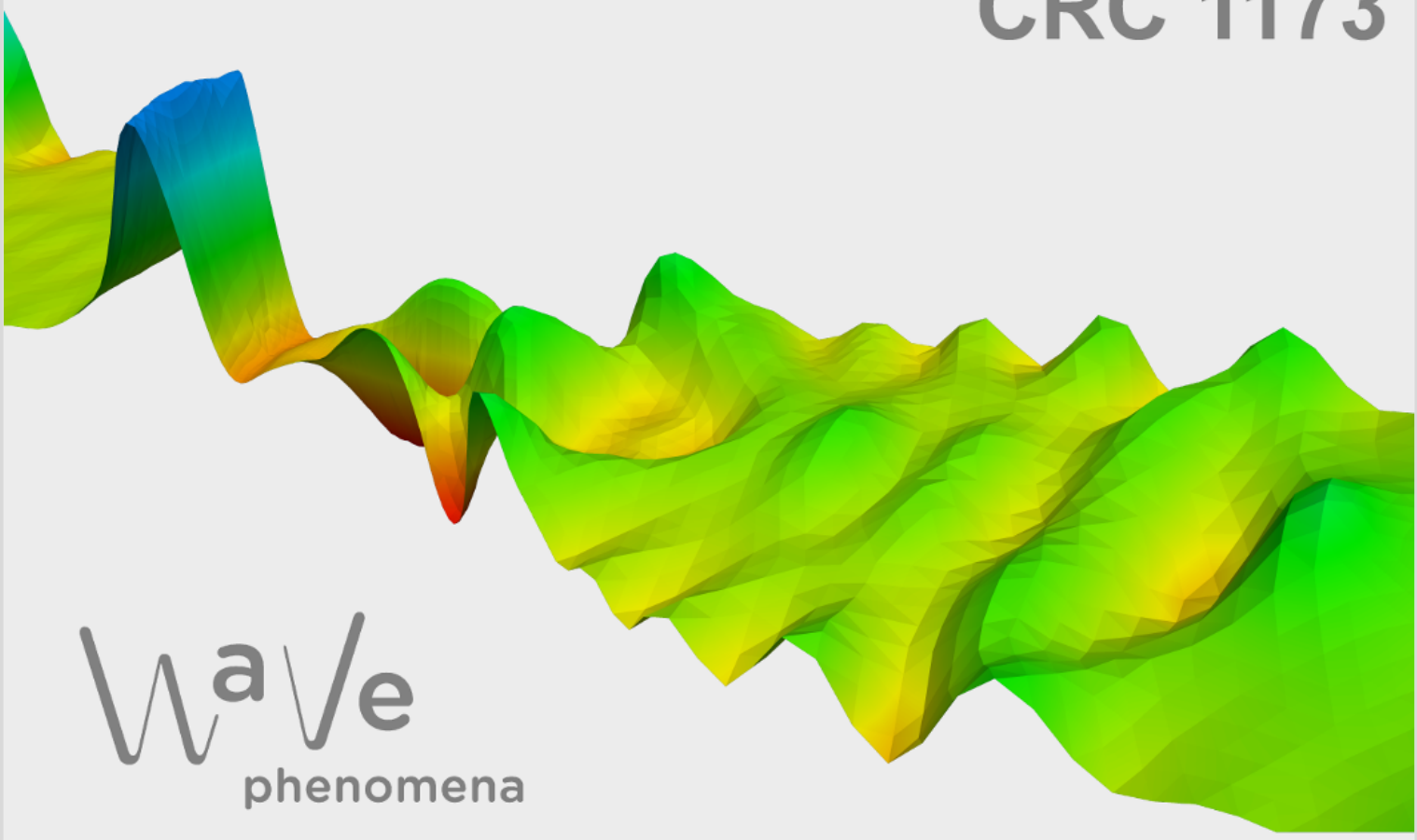

Participating universities

Funded by

ISSN 2365-662X

LEAPFROG CRANK–NICOLSON DECOUPLING OF WAVE-HEAT-TYPE PROBLEMS

BENJAMIN DÖRICH AND JULIAN DÖRNER

Abstract. This paper proposes and analyzes a numerical method for coupled wave–heat systems that arise, for example, in viscoelasticity with memory, thermoelastic wave propagation with finite thermal speed, and Maxwell's equations coupled to dispersive material laws. Motivated by the widespread use of explicit leapfrog schemes for wave problems and the parabolic time-step restriction for heat equations, we design a second-order scheme that combines leapfrog time integration for the wave part with a Crank–Nicolson step for the heat part. The coupling is arranged in a Strang-splitting–type fashion so that the overall scheme remains explicit in the coupling and is subject only to a CFL condition of hyperbolic type, rather than the more restrictive parabolic constraint.

We introduce an abstract space discretization that covers a broad class of wave–heat systems and accommodates both conforming and stabilized nonconforming discretizations. Using an extended unified error decomposition, we derive error estimates for the fully discrete scheme under the desired CFL condition. Numerical experiments for our model applications confirm the theoretical results.

1. Introduction

In this paper we study wave-type systems which are coupled to heat-type problem and can formally be written as

$$\partial_t x + Sx = -\widetilde{B}\theta + f, \tag{1.1a}$$

$$\partial_t \theta + L\theta = \widetilde{B}^* x + g, \tag{1.1b}$$

where the wave part (1.1a) is given as a two-component system with $x = (x_1, x_2) \in X = X_1 \times X_2$ and a skew-adjoint operator S, and some dissipative operator L in (1.1b).

In this work we have four main classes of examples in mind. As a particularly simple and illustrative starting point, we first consider a one-dimensional wave equation coupled to a heat equation, modeling a thermoelastic string.

A second example is given by nonlocal-in-time linear viscoelasticity systems, which describe materials with memory effects subject to pressure and shear waves.

As a third example, we consider thermoelastic wave equations, which model the coupled propagation of mechanical and thermal disturbances in a solid and, in

2020 *Mathematics Subject Classification.* Primary 65M12, 65M15, 65M60; Secondary 35Q60, 35Q74, 74F05.

Key words and phrases. leapfrog scheme; Crank–Nicolson scheme; CFL condition; stability; a priori error estimates; coupled hyperbolic–parabolic systems.

The authors acknowledge funding by the Deutsche Forschungsgemeinschaft (DFG, German Research Foundation) through the Project-ID 258734477 – SFB 1173.

contrast to classical Fourier heat conduction, account for a finite propagation speed of thermal signals. Compare [KGBB79] and [IOS10] for a general introduction.

Finally, we consider Maxwell's equations in a bulk medium coupled to a system of differential equations posed on an interface, modeling the nonlocal-in-time response of an artificial two-dimensional metamaterial such as graphene.

To be more precise, all our examples fit in the more specific structure of (1.1), i.e.

$$\partial_t x_1 - S_2 x_2 = -B\theta + f_1 \tag{1.2a}$$

$$\partial_t x_2 + S_1 x_1 = 0 \tag{1.2b}$$

$$\partial_t \theta + L\theta = B^* x_1 + g. \tag{1.2c}$$

In the applications, the leapfrog scheme is the favorite method to discretize the (spatially discrete) wave problem. It is explicit and preserves important geometric properties of the solution. However, this scheme comes with a CFL-condition which roughly speaking only allows for time steps τ in the order of the mesh size h. While this is widely accepted to be still competitive, this becomes different if an explicit scheme is applied to a heat-type problem as well, since here a scaling as $\tau \lesssim h^2$ is usually required. Thus, we propose to combine the leapfrog method for the wave part with the implicit Crank–Nicolson method for the heat part in order to solve the problem only under the weaker CFL condition. Formal application of the scheme to a finite dimensional version of (1.2) reads

$$x_1^{n+1/2} = x_1^n + \frac{\tau}{2} S_2 x_2^n - \frac{\tau}{2} B\theta^n + \frac{\tau}{2} f_1^n, \tag{1.3a}$$

$$x_2^{n+1} = x_2^n - \tau S_1 x_1^{n+1/2}, \tag{1.3b}$$

$$\theta^{n+1} = \theta^n - \frac{\tau}{2} L\big(\theta^{n+1} + \theta^n\big) + \tau B^* x_1^{n+1/2} + \frac{\tau}{2}\big(g^{n+1} + g^n\big), \tag{1.3c}$$

$$x_1^{n+1} = x_1^{n+1/2} + \frac{\tau}{2} S_2 x_2^{n+1} - \frac{\tau}{2} B\theta^{n+1} + \frac{\tau}{2} f_1^{n+1}, \tag{1.3d}$$

at times $t_n = n\tau + t_0$, for $n \geq 0$ subject to suitable initial values (x^0, θ^0). Equations (1.3a), (1.3b), and (1.3d) constitute the standard leapfrog scheme applied to the wave equation (1.2a), (1.2b), with the heat variable entering as an additional source term. Equation (1.3c) is a Crank–Nicolson step for the heat variable, where the source term arising from the wave coupling is evaluated at the temporal midpoint in order to keep the overall coupling of both time-integration schemes explicit. Thus, our scheme has the flavor of a Strang splitting scheme, solving both problems interlaced with suitable schemes for every sub-problem.

Since the application of an explicit scheme is not suitable on the operator level, we discretize in space first. We present our discretization in an abstract manner in order to cover the four examples mentioned above in a unified framework. In particular, we allow for conforming and non-conforming discretizations in the wave part. For the spatially discrete error analysis, we follow the ideas of [HHS19] and collect the different error contributions in a decomposition which allows for direct application of results form the literature to derive the optimal error bounds. We emphasize here, that we allow for stabilized non-conforming discretizations, and, thus, extend the unified framework in [HHS19] about this important class of space discretization schemes. The fully discrete scheme can then be analyzed as a perturbation of the Crank–Nicolson method, however one can attribute a sign to the perturbation, which allows for a stable scheme under the desired CFL condition

$\tau \lesssim h$. Further, let us note that we employ summation-by-parts in order to avoid unphysical constraints on the right-hand sides.

To the best of our knowledge, there is hardly any work on the decoupling strategies of wave-heat type problems, apart from [LT12]. There, the stability of two second-order two-step methods is analyzed. However, the analysis is restricted to ordinary differential equations and does not provide any error bounds.

Nevertheless, there is a large literature available for the individual examples, and we provide a non-exhaustive short overview of results in the following:

In the context of visco-elastic waves, an upwind-flux stabilized discontinuous Galerkin method is a well-established scheme in geophysics, cf. [KD06, DK06]. For time-integration, implicit Runge-Kutta schemes are discussed in [HPS$^+$15], as well as space-times methods in [DFW16, DWZ19].

In the case of linear thermo-elasticity, various numerical and analytical approaches have been proposed in the literature. Boundary element methods for coupled thermo-elastic problems in a scattering setting are investigated in [HSVSW19], while in [JR00] the problem is formulated and studied in the framework of abstract evolution equations. Furthermore, qualitative stability properties for thermo-elastic systems are analyzed in [BGN14].

For the Maxwell problem with discontinuous Galerkin discretization in space there are the seminal works by Hesthaven & Warburton [HW02] and Fezoui et al. [FLLP05], which lay the foundation for the time-domain Maxwell problem. A generalization to dispersive media, which has structural similarities to our model, was provided by Lanteri & Scheid [LS13], and more recently the authors laid the foundation for the treatment of the interface problem in [DDH26].

The rest of the paper is organized as follows: In Section 2, we introduce the analytical framework as well as the above-mentioned examples that fit into this framework. We then introduce the abstract spatial discretization in Section 3, and provide a semi-discrete error bound. In Section 4, we derive our fully discrete method, provide stability estimates, and show convergence of optimal order. Section 5 is devoted to our examples. We discuss the spatial discretization in the specific settings and apply our main results. Our numerical experiments in Section 6 confirm the theoretical findings. Some computations are postponed to the Appendix A.

Notation. Throughout this work, we denote by $L^2(\Omega)$ the standard Lebesgue space of square integrable functions on a domain Ω. The standard Sobolev spaces of order $k \geq 0$ are denoted with $H^k(\Omega)$, as well as its closed subspace $H^1_0(\Omega)$ with vanishing trace. Further, we use the standard spaces for the weak divergence $H(\mathrm{div})$, together with its closed subspaces $H_0(\mathrm{div})$, i.e. $\boldsymbol{v} \cdot \nu = 0$ on $\partial\Omega$ for all $\boldsymbol{v} \in H_0(\mathrm{div})$. For a Hilbert space X, we denote its topological dual by X^* together with the induced norm. In addition, we write $\alpha \lesssim \beta$ if there is a constant C independent of the spatial mesh parameter h and the time step size τ such that $\alpha \leq C\beta$.

2. Analytical framework and main examples

We first discuss the analytical framework for the rest of the paper. For a rigorous treatment we move to a weak formulation of (1.1). Before we present the equation, we introduce the two Gelfand triples

$$Y \hookrightarrow X \hookrightarrow Y^*, \qquad V \hookrightarrow H \hookrightarrow V^*$$

with dense embeddings, belonging to the wave and heat part, respectively. On these spaces, we consider the bilinear forms

$$p\colon X \times X \to \mathbb{R}, \quad s\colon Y \times Y \to \mathbb{R},$$
$$\widetilde{p}\colon H \times H \to \mathbb{R}, \quad \widetilde{s}\colon V \times V \to \mathbb{R},$$

where p and $\widetilde{p}$ are simply the inner products of X and H, respectively, and s and $\widetilde{s}$ encode the differential operators. Further, we introduce the coupling form

$$\widetilde{b}\colon V \times Y \to \mathbb{R}\,.$$

In order to resemble the two-field structure of the wave part, cf. eq. (1.2), we assume that the bilinear form p and s can be decomposed as

$$p(x,y) = p_1(x_1,y_1) + p_2(x_2,y_2), \qquad s(x,y) = s_1(x_1,y_2) - s_2(x_2,y_1),$$

and the coupling as well as the forcing only appears in the first component of the wave system as

$$\widetilde{b}(\theta,y) = b(\theta,y_1), \qquad p(f,y) = p_1(f_1,y_1), \tag{2.1}$$

With this, we can formulate problem (1.1) as follows:

Seek $x \in C^1(\mathbb{R},X) \cap C(\mathbb{R},Y)$ and $\theta \in C^1(\mathbb{R},H) \cap C(\mathbb{R},V)$ which satisfy

$$p(\partial_t x, y) + s(x,y) = -\widetilde{b}(\theta,y) + p(f,y) \tag{2.2a}$$

$$\widetilde{p}(\partial_t \theta, \varphi) + \widetilde{s}(\theta,\varphi) = \widetilde{b}(\varphi,x) + \widetilde{p}(g,\varphi), \tag{2.2b}$$

for all $y \in Y$ and $\varphi \in V$, as well as the initial conditions $x(0) = x_0$ and $\theta(0) = \theta_0$. For the analysis, we make the following assumptions, which are verified later on for our individual examples.

Assumption 2.1. (a) The bilinear forms p and $\widetilde{p}$ are scalar products and induce the norms

$$\|y\|_X^2 = p(y,y) \quad \text{and} \quad \|\varphi\|_H^2 = \widetilde{p}(\varphi,\varphi),$$

for any $y \in X$ and $\varphi \in H$.
(b) It holds that

$$s(y,y) = 0 \quad \text{and} \quad \widetilde{s}(\varphi,\varphi) \geq 0$$

for $y \in Y$ and $\varphi \in V$.
(c) There exist spaces $\mathcal{Z} \subset \mathcal{Z}_1 \times \mathcal{Z}_2 \subset Y \times V$ and bilinear forms $\widehat{s}\colon \mathcal{Z}_1 \times X$ and $\widehat{b}\colon \mathcal{Z}_2 \times X$ such that it holds

$$s(x,y) + \widetilde{b}(\theta,y) = \widehat{s}(x,y) + \widehat{b}(\theta,y)$$

for all $(x,\theta) \in \mathcal{Z}$ and $y \in Y$.

Remark 2.2. The rather technical assumption in part (c) allows for coupling operators that do not act in the bulk but via an interface or boundary. Such a coupling can be expressed indirectly via partial integration, which motivates our assumption. A concrete examples is given later in Section 2.4.

Let us also emphasize that part (c) implies that a solution (x,θ) of (2.2) which is continuous in $\mathcal{Z}$ also satisfies

$$p(\partial_t x, y) + \widehat{s}(x,y) = -\widehat{b}(\theta,y) + p(f,y) \tag{2.3}$$

for all $y \in X$ using a density argument. We also note that with some additional notation, one could also treat a dissipative wave-type problem, i.e. $s(y,y) \geq 0$.

This framework immediately allows for the following a-priori stability result.

Lemma 2.3. *Let $x \in C^1([0,T],X)\cap C([0,T],Y)$ and $\theta \in C^1([0,T],H)\cap C([0,T],V)$ be a solution of (2.2), then*

$$\|x(t)\|_X^2 + \|\theta(t)\|_H^2 \le e\big(\|x(0)\|_X^2 + \|\theta(0)\|_H^2\big) + eT\Big(\int_0^t \|f(s)\|_X^2 + \|q(s)\|_H^2\, ds\Big).$$

Proof. To obtain this result, we test with the solution in (2.2), apply Cauchy-Schwarz as well as a (time-)weighted Young inequality, and conclude via the Gronwall lemma in [Emm99, Proposition 2.1]. □

Remark 2.4. We could also allow for nonlinear contributions f or g in (2.2), which are locally Lipschitz in X or H, respectively. However, since this does not change the analysis in an essential manner, we omit this here for the sake of presentation.

In the following sections, we discuss the examples from the introduction and show how they fit into the framework from above.

2.1. **Thermoelastic string.** Our first example concerns the modelling of a string on an interval $\Omega = (a,b)$ with displacement u subject to a heating field θ, see for example Section 3.3.1 in [BGN14]. The governing equations read

$$\partial_t^2 u - \partial_x^2 u = -\partial_x \theta + f, \tag{2.4a}$$

$$\partial_t \theta - \partial_x^2 \theta = -\partial_x \partial_t u + g. \tag{2.4b}$$

In order to fit this problem into our general framework, we have to make the (unusual) definition $x = (\partial_t u, u)$. If we want to change the positions, we simply have to change the roles of the first and second component of x in the rest of this work. Consequently, we define the spaces

$$X = L^2(\Omega)\times H_0^1(\Omega), \quad Y = H_0^1(\Omega)\times H_0^1(\Omega), \qquad H = L^2(\Omega), \quad V = H_0^1(\Omega),$$

as well as the forms

$$p(\cdot,\cdot) = \langle\cdot,\cdot\rangle_{L^2\times H_0^1}, \quad s_1(x_1,y_2) = -\langle\partial_x x_1, \partial_x y_2\rangle_{L^2}, \quad s_2(x_2,y_1) = s_1(x_2,y_1),$$
$$\widetilde{p}(\cdot,\cdot) = \langle\cdot,\cdot\rangle_{L^2}, \qquad \widetilde{s}(\cdot,\cdot) = \langle\cdot,\cdot\rangle_{H_0^1},$$

such that part (a) and (b) of Assumption 2.1 are satisfied. Further, we define the coupling form

$$\widetilde{b}(\varphi, x) = \langle\varphi, \partial_x\partial_t u\rangle_{L^2},$$

and observe that the extended bilinear forms in Assumption 2.1 (c) can be chosen to be the original ones.

2.2. **Non-local in time visco-elasticity and acoustics.** In our second example we treat wave propagation in visco-elastic solids and its acoustic analogue. We begin with the visco-elastic wave equations, i.e., elastic waves in solids subject to non-local in time material laws.

Let $\Omega \subset \mathbb{R}^d$, $d \in \{2,3\}$, denote the spatial domain. We denote by $\boldsymbol{v}$ the velocity field and by $\boldsymbol{\sigma}_i$ the symmetric stress tensors corresponding to different relaxation mechanisms, $i = 0,\dots,G$. The strain-rate tensor is given by $\epsilon(\boldsymbol{v}) = \mathrm{Sym}(D\boldsymbol{v})$.

They satisfy the system

$$\rho\partial_t \boldsymbol{v} - \operatorname{div} \boldsymbol{\sigma}_0 = \sum_{i=1}^{G} \operatorname{div} \boldsymbol{\sigma}_i + f, \tag{2.5a}$$

$$C_0^{-1}\partial_t \boldsymbol{\sigma}_0 - \epsilon(\boldsymbol{v}) = 0, \tag{2.5b}$$

$$C_i^{-1}\partial_t \boldsymbol{\sigma}_i + (C_i\tau_i)^{-1}\boldsymbol{\sigma}_i = \epsilon(\boldsymbol{v}), \qquad i = 1, \dots, G. \tag{2.5c}$$

To fit this problem into our abstract framework, we split the unknowns in

$$x = (\boldsymbol{v}, \boldsymbol{\sigma}_0), \qquad \theta = (\boldsymbol{\sigma}_1, \dots, \boldsymbol{\sigma}_G),$$

and choose the spaces

$$\begin{aligned} X &= L^2(\Omega)^{(d+1)d}, \quad Y = H_0^1(\Omega, \mathbb{R}^d) \times H(\operatorname{div}, \Omega, \mathbb{R}^{d\times d}_{\mathrm{sym}}), \\ H &= L^2(\Omega)^{Gd^2}, \qquad V = H(\operatorname{div}, \Omega, \mathbb{R}^{d\times d}_{\mathrm{sym}})^G. \end{aligned}$$

For $x = (\boldsymbol{v}, \boldsymbol{\sigma}_0)$, $y = (\boldsymbol{w}, \widetilde{\boldsymbol{\sigma}_0})$ and $\theta = (\boldsymbol{\sigma}_1, \dots, \boldsymbol{\sigma}_G)$ we define

$$\begin{aligned} p(x, y) &= \langle \rho\boldsymbol{v}, \boldsymbol{w}\rangle_{L^2} + \langle C_0^{-1}\boldsymbol{\sigma}_0, \widetilde{\boldsymbol{\sigma}_0}\rangle_{L^2}, \\ s(x, y) &= -\langle \operatorname{div} \boldsymbol{\sigma}_0, \boldsymbol{w}\rangle_{L^2} - \langle \epsilon(\boldsymbol{v}), \widetilde{\boldsymbol{\sigma}_0}\rangle_{L^2}, \\ \widetilde{p}(\theta, \widehat{\theta}) &= \sum_{i=1}^{G} \langle C_i^{-1}\boldsymbol{\sigma}_i, \widehat{\boldsymbol{\sigma}}_i\rangle_{L^2}, \\ \widetilde{s}(\theta, \widehat{\theta}) &= \sum_{i=1}^{G} \langle (C_i\tau_i)^{-1}\boldsymbol{\sigma}_i, \widehat{\boldsymbol{\sigma}}_i\rangle_{L^2}, \end{aligned}$$

and the coupling form

$$\widetilde{b}(\theta, x) = -\sum_{i=1}^{G} \langle \operatorname{div} \boldsymbol{\sigma}_i, \boldsymbol{v}\rangle_{L^2} = \sum_{i=1}^{G} \langle \boldsymbol{\sigma}_i, \epsilon(\boldsymbol{v})\rangle_{L^2},$$

where the second equality follows from integration by parts and the homogeneous boundary conditions. Note that the extended bilinear forms in Assumption 2.1 (c) can be chosen to be the original ones.

A scalar visco-acoustic analogue of this model is obtained by replacing the tensor-valued stresses $\boldsymbol{\sigma}_i$ by scalar pressures p_i, $i = 0, \dots, G$, and the shear modulus by the bulk modulus κ. This leads to the system

$$\rho\partial_t \boldsymbol{v} - \nabla p_0 = \sum_{i=1}^{G} \nabla p_i + f, \tag{2.6a}$$

$$\kappa^{-1}\partial_t p_0 - \operatorname{div} \boldsymbol{v} = 0, \tag{2.6b}$$

$$(\kappa\tau_P)^{-1}\partial_t p_i + (\kappa\tau_P\tau_i)^{-1} p_i = \operatorname{div} \boldsymbol{v}, \qquad i = 1, \dots, G. \tag{2.6c}$$

To fit (2.6) into our framework, we again split

$$x = (\boldsymbol{v}, p_0), \qquad \theta = (p_1, \dots, p_G),$$

and choose

$$\begin{aligned} X &= L^2(\Omega)^{d+1}, \quad Y = H_0(\operatorname{div}, \Omega, \mathbb{R}^d) \times H^1(\Omega), \\ H &= L^2(\Omega)^G, \qquad V = H^1(\Omega)^G. \end{aligned}$$

For $x = (\boldsymbol{v}, p_0)$, $y = (\boldsymbol{w}, q_0)$ we set

$$\begin{aligned} p(x,y) &= \langle \rho \boldsymbol{v}, \boldsymbol{w} \rangle_{(L^2)^d} + \langle \kappa^{-1} p_0, q_0 \rangle_{L^2}, \\ s(x,y) &= -\langle \nabla p_0, \boldsymbol{w} \rangle_{L^2} - \langle \operatorname{div} \boldsymbol{v}, q_0 \rangle_{L^2}, \\ \widetilde{p}(\theta, \widehat{\theta}) &= \langle (\kappa \tau_P)^{-1} \theta, \widehat{\theta} \rangle_{(L^2)^G}, \\ \widetilde{s}(\theta, \widehat{\theta}) &= \sum_{i=1}^{G} \langle (\kappa \tau_P \tau_i)^{-1} p_i, \widehat{p}_i \rangle_{L^2}, \end{aligned}$$

and the coupling form

$$\widetilde{b}(\theta, x) = -\sum_{i=1}^{G} \langle \nabla p_i, \boldsymbol{v} \rangle_{L^2}.$$

Again, the extended bilinear forms in Assumption 2.1 (c) can be chosen to be the original ones.

2.3. **Thermo-elastic wave coupling.** Our third example concerns elastic solids coupled with heat conduction.

Let $\Omega \subset \mathbb{R}^d$, $d \in \{2, 3\}$, be the spatial domain. We consider the displacement field $\boldsymbol{u}$ and the scalar temperature distribution θ, which satisfy the linear thermo-elastic system

$$\begin{aligned} \rho \partial_t^2 \boldsymbol{u} - \mu \Delta \boldsymbol{u} - (\lambda + \mu) \nabla (\operatorname{div} \boldsymbol{u}) &= \alpha \nabla \theta + \rho f, \\ \partial_t \theta - \kappa \Delta \theta &= \alpha \operatorname{div}(\partial_t \boldsymbol{u}) + h, \end{aligned}$$

with Lamé parameters $\lambda \geq 0$, $\mu > 0$, coupling parameter $\alpha > 0$, and thermal diffusivity $\kappa > 0$. We rewrite the system in terms of the velocity $\boldsymbol{v} = \partial_t \boldsymbol{u}$ and the symmetric stress $\boldsymbol{\sigma}$, to obtain

$$\rho \partial_t \boldsymbol{v} - \operatorname{div} \boldsymbol{\sigma} = \alpha \nabla \theta + \rho f, \tag{2.7a}$$

$$\partial_t \boldsymbol{\sigma} - C\, \epsilon(\boldsymbol{v}) = 0, \tag{2.7b}$$

$$\partial_t \theta - \kappa \Delta \theta = \alpha \operatorname{div} \boldsymbol{v} + h, \tag{2.7c}$$

where $C\boldsymbol{w} = 2\mu \boldsymbol{w} + \frac{1}{3} \operatorname{tr}(\boldsymbol{w}) I$ is the isotropic elasticity tensor and $\epsilon(\boldsymbol{v}) = \operatorname{sym}(D\boldsymbol{v})$ the symmetric gradient.

To fit (2.7) into our abstract framework, we collect the mechanical unknowns in $x = (\boldsymbol{v}, \boldsymbol{\sigma})$ and treat the temperature as the "heat part" θ. We choose the spaces

$$\begin{aligned} X &= L^2(\Omega)^{d(d+1)}, \quad & Y &= H_0^1(\Omega, \mathbb{R}^d) \times H^1(\operatorname{div}, \Omega, \mathbb{R}^{d \times d}_{\operatorname{sym}}), \\ H &= L^2(\Omega), & V &= H_0^1(\Omega). \end{aligned}$$

For $x = (\boldsymbol{v}, \boldsymbol{\sigma})$ and $y = (\widetilde{\boldsymbol{v}}, \widetilde{\boldsymbol{\sigma}})$ we define

$$\begin{aligned} p(x,y) &= \langle \rho \boldsymbol{v}, \widetilde{\boldsymbol{v}} \rangle_{(L^2)^d} + \langle C^{-1} \boldsymbol{\sigma}, \widetilde{\boldsymbol{\sigma}} \rangle_{(L^2)^{d \times d}}, & s(x,y) &= -\langle \operatorname{div} \boldsymbol{\sigma}, \widetilde{\boldsymbol{v}} \rangle_{L^2} - \langle \epsilon(\boldsymbol{v}), \widetilde{\boldsymbol{\sigma}} \rangle_{L^2}, \\ \widetilde{p}(\theta, \widehat{\theta}) &= \langle \theta, \widehat{\theta} \rangle_{L^2}, & \widetilde{s}(\theta, \widehat{\theta}) &= \langle \kappa \nabla \theta, \nabla \widehat{\theta} \rangle_{L^2}, \end{aligned}$$

and the coupling form

$$\widetilde{b}(\theta, x) = -\langle \alpha \nabla \theta, \boldsymbol{v} \rangle_{L^2}.$$

As in the previous examples, the extended bilinear forms in Assumption 2.1 (c) can be chosen to be the original ones.

2.4. **Maxwell equation with dissipative 2D material.** Our last example models the light-matter interaction of thin, two-dimensional metamaterials, like graphene. For the sake of presentation, we omit any physical constants.

Let $\Omega = (-1,1)\times(0,1)^2$ denote a rectangular domain, partitioned by an interface F_{int} such that

$$\Omega_1 = (-1,0)\times(0,1)^2, \quad \Omega_2 = (0,1)\times(0,1)^2, \quad F_{\text{int}} = \{0\}\times(0,1)^2.$$

Besides the electric and magnetic field E and H, defined on Ω_i, we further have a set of auxiliary fields $(\theta_1,\dots,\theta_\ell)$ on the interface F_{int} with values parallel to the interface. The governing equations read

$$\partial_t E - \operatorname{curl} H = J, \qquad \text{in } [0,T]\times\Omega_i, \tag{2.8a}$$

$$\partial_t H + \operatorname{curl} E = 0, \qquad \text{in } [0,T]\times\Omega_i, \tag{2.8b}$$

$$\partial_t \theta + L\theta = \mathbb{1}_\ell \otimes E_\parallel + g, \qquad \text{on } [0,T]\times F_{\text{int}}, \tag{2.8c}$$

where $E_\parallel$ is the tangential projection of E onto F_{int}, the matrix $L \in \mathbb{R}^{2\ell\times 2\ell}$ is symmetric and positive definite, and $\mathbb{1}_\ell$ is the ℓ-dimensional one vector.

In order to close the system described by (2.8), a coupling of the auxiliary variables into the Maxwell system needs to be described. This is formally given by the interface condition

$$[\![H\times n_{\text{int}}]\!]_{F_{\text{int}}} = -(\mathbb{1}_\ell^T \otimes I_2)\theta, \tag{2.8d}$$

where $I_2 = \operatorname{diag}(1,1)$, the vector n_{int} denotes the unit normal on F_{int}, and the double bracket the jump at the interface. The latter condition has to be carefully included into the system via the domain of the operators since the coupling is not described by an operator defined on the bulk. We will further elaborate on this at the end of the section.

To fit this problem into our abstract framework, we set $x = (x_1,x_2) = (E,H)$ and use the spaces

$$\begin{aligned} X &= L^2(\Omega)^6, \quad Y = H_0^{\text{imp}}(\operatorname{curl}) \times H^{\text{imp}}(\widetilde{\operatorname{curl}}),\\ H &= V = L^2(F_{\text{int}})^{2\ell}, \quad \ell\in\mathbb{N}_+, \end{aligned}$$

with the regularized curl-spaces

$$\begin{aligned} H_0^{\text{imp}}(\operatorname{curl}) &= \{\, E\in L^2(\Omega)^3 \mid \operatorname{curl} E \in L^2(\Omega)^3,\ E_\parallel \in L^2(F_{\text{int}})^2,\ E\times\nu = 0\,\},\\ H^{\text{imp}}(\widetilde{\operatorname{curl}}) &= \{\, H\in L^2(\Omega)^3 \mid \widetilde{\operatorname{curl}}\, H \in L^2(\Omega)^3,\ [\![H\times n]\!]_{F_{\text{int}}} \in L^2(F_{\text{int}})^2\,\}. \end{aligned}$$

Here, $\widetilde{\operatorname{curl}}$ denotes a piecwise curl, i.e. for $E\in L^2(\Omega)^3$ we define

$$\widetilde{\operatorname{curl}}\, E \in L^2(\Omega)^3 \quad \Leftrightarrow \quad \operatorname{curl} E\big|_{\Omega_i} \in L^2(\Omega_i)^3,\ i\in\{1,2\}.$$

For any details on those spaces and the resulting traces we refer to [ACL18, Sec. 2.2.2]. Finally, we define the forms

$$\begin{aligned} p(\cdot,\cdot) &= \langle\cdot,\cdot\rangle_{L^2(\Omega)^6},\\ \widetilde{p}(\cdot,\cdot) &= \langle\cdot,\cdot,\cdot\rangle_{L^2(F_{\text{int}})^{2\ell}},\\ s(x,y) &= -p(\operatorname{curl} x_1, y_2) + p(x_2, \operatorname{curl} y_1),\\ \widetilde{s}(\theta,\varphi) &= \widetilde{p}(L\theta,\varphi), \end{aligned}$$

with coupling form

$$\widetilde{b}(\varphi, x) = \widetilde{p}(\varphi, \mathbb{1}_\ell \otimes x_{1,\|}).$$

Standard results yield that part (a) and (b) of Assumption 2.1 are satisfied.

As mentioned before, we include condition (2.8d) in the operator domain and define

$$\mathcal{Z} = Y \times V \cap \{[\![x_2 \times n_{\mathrm{int}}]\!]_{F_{\mathrm{int}}} = -(\mathbb{1}_\ell^T \otimes I_2)\theta\},$$

together with the extended forms

$$\widehat{b} \equiv 0, \qquad \widehat{s}(x, y) = p(\operatorname{curl} x_1, y_2) - p(\widetilde{\operatorname{curl}}\, x_2, y_1).$$

Assumption 2.1 (c) is now an integration-by-parts formula, describing the interplay of the piecewise defined fields and the definition of the domain $\mathcal{Z}$. It is obtained by applying [ACL18, Thm. 2.2.18] piecewise on both sub-domains together with a density argument.

3. Spatial discretization

We now turn to the discretization of (2.2) in space. We therefore consider the finite dimensional spaces Y_h and V_h for the discrete wave function x_h and discrete heat function θ_h. Since we do not only consider conforming methods for the wave problem, we do not assume the discrete spaces Y_h to be a subspaces of Y, but only

$$Y_h \subset X \quad \text{and} \quad V_h \subset V. \tag{3.1}$$

In addition, we also use the subspaces with the weaker norms induced by p and $\widetilde{p}$ and denote them by X_h and H_h, respectively. Thus, we can keep the forms p, $\widetilde{p}$ and $\widetilde{s}$ for the spatial discretization and only focus on the discrete counterparts of s and $\widetilde{b}$. We consider

$$s_h \colon (Y + Y_h) \times (Y + Y_h) \to \mathbb{R}, \qquad \widetilde{b}_h \colon H_h \times (Y + Y_h) \to \mathbb{R}\,,$$

and can thus formulate the semi discrete problem as follows:

Seek $x_h \in C^1([0,T], Y_h)$ and $\theta_h \in C^1([0,T], V_h)$ such that

$$p(\partial_t x_h, y_h) + s_h(x_h, y_h) = -\widetilde{b}_h(\theta_h, y_h) + p(f_h, y_h), \tag{3.2a}$$

$$\widetilde{p}(\partial_t \theta_h, \varphi_h) + \widetilde{s}(\theta_h, \varphi_h) = \widetilde{b}_h(\varphi_h, x_h) + \widetilde{p}(g_h, \varphi_h), \tag{3.2b}$$

holds for all $y_h \in Y_h$ and $\varphi_h \in V_h$ with initial conditions $x_h(0) = x_{h,0}$ and $\theta_h(0) = \theta_{h,0}$.

Remark 3.1. We could also treat the more general case of a non-conforming method for the heat part, where the second part of (3.1) is not satisfied, for example using mass lumping or symmetric interior penalty dG for the heat part. However, this only leads to a repetition of the arguments from the wave part, and we thus omit this for the sake of readability.

In the following, we make two structural assumptions on the discrete form for the wave part. The first one guarantees that up to a stabilization term, the skew-adjointness is preserved. Furthermore, we assume that the stabilization only acts on discrete functions.

Assumption 3.2. (a) The discrete form s_h can be decomposed in a skew-symmetric and positive (stabilization) part as $s_h = s_h^s + s_h^p$ which satisfy

$$s_h^s(y_h, y_h) = 0, \qquad s_h^p(y_h, y_h) \geq 0$$

for all $y_h \in Y_h$.

(b) For all $y \in Y$, the stabilization vanishes, i.e.,

$$s_h^p(y, y_h) = 0$$

for all $y_h \in Y_h$.

The next assumption is a consistency condition which allows us to incorporate coupling information of the wave part from the domain into the error analysis via integration by parts, see Remark 2.2.

Assumption 3.3. For $(x, \theta) \in \mathcal{Z}$ and $y_h \in X_h$ it holds the generalized consistency condition

$$s_h(x, y_h) + \widetilde{b}_h(\theta, y_h) = \widehat{s}(x, y_h) + \widehat{b}(\theta, y_h),$$

where $\widehat{s}$ and $\widehat{b}$ are defined in Assumption 2.1.

The positive part in our discretization stems from numerical stabilization such as upwinding, commonly used with discontinuous Galerkin methods. We associate with it a semi-norm $|y_h|_{s_h^p}^2 = s_h^p(y_h, y_h)$ and note, due to the skew-adjointness, the relation

$$s_h(y_h, y_h) = |y_h|_{s_h^p}^2. \tag{3.3}$$

For the best approximation result, we further require several projections into the discrete spaces. We consider the orthogonal projections

$$P_h \colon X \to Y_h, \quad \widetilde{P}_h \colon H \to V_h,$$

with respect to the inner products p and $\widetilde{p}$, respectively, and also the reference operators

$$J_h \colon Y \to Y_h \quad \widetilde{J}_h \colon V \to V_h.$$

In the spirit of [HHS19], we define the following errors terms in order to keep track of the different contributions and to estimate them for the specific examples:

$$\Delta p(x, y_h) = p(J_h x - x, y_h), \tag{3.4a}$$

$$\Delta_{s,b}(x, \theta, y_h) = s_h(J_h x, y_h) + \widetilde{b}_h(\widetilde{J}_h \theta, y_h) - \widehat{s}(x, y_h) - \widehat{b}(\theta, y_h), \tag{3.4b}$$

$$\Delta f(y_h) = p(f_h - f, y_h), \tag{3.4c}$$

$$\Delta \widetilde{p}(\theta, \varphi_h) = \widetilde{p}(\widetilde{J}_h \theta - \theta, \varphi_h), \tag{3.4d}$$

$$\widetilde{\Delta}_{s,b}(x, \theta, \varphi_h) = \widetilde{s}(\widetilde{J}_h \theta - \theta, \varphi_h) - \widetilde{b}_h(\varphi_h, J_h x) + \widetilde{b}(\varphi_h, x), \tag{3.4e}$$

$$\Delta g(\varphi_h) = \widetilde{p}(g_h - g, \varphi_h). \tag{3.4f}$$

Here, the errors in (3.4a) and (3.4d) constitute best-approximation errors, the terms (3.4b) and (3.4e) contain the approximation of the differential and coupling operators, and (3.4c) and (3.4f) describe the approximation of the right-hand sides. This, allows us to formulate the following abstract error result for the discrete errors

$$e_h(t) = J_h x(t) - x_h(t), \qquad \epsilon_h(t) = \widetilde{J}_h \theta(t) - \theta_h(t). \tag{3.5}$$

The full error is then decomposed in the discrete error and some best-approximation error.

Theorem 3.4. *Let $x \in C^1([0,T],Y)$ and $\theta \in C^1([0,T],V)$ be the solution of (2.2), which satisfies $(x,\theta) \in C^1([0,T],\mathcal{Z})$, and (x_h,θ_h) the solution of (3.2). Further, let Assumptions 2.1, 3.2, and 3.3 hold true. Then, the errors defined in (3.5) satisfy*

$$\begin{aligned}
&\|e_h(t)\|_{X_h}^2 + \|\epsilon_h(t)\|_{H_h}^2 + \int_0^t |e_h(t)|_{s_h^p}^2 \, ds \\
&\quad \lesssim \|e_h(0)\|_{X_h}^2 + \|\epsilon_h(0)\|_{X_h}^2 + \int_0^t \|\Delta p(\partial_t x)\|_{X_h^*}^2 + \|\Delta \widetilde{p}(\partial_t \theta)\|_{H_h^*}^2 \, ds \\
&\qquad + \int_0^t |\Delta_{s,b}(x,\theta,e_h)| + \|\widetilde{\Delta}_{s,b}(x,\theta)\|_{H_h^*}^2 \, ds + \int_0^t \|\Delta f\|_{X_h^*}^2 + \|\Delta g\|_{H_h^*}^2 \, ds
\end{aligned}$$

with constants independent of h.

We note that in order to later treat upwinded schemes, we have to leave the term $\Delta_{s,b}$ on the right-hand side, since, depending on the chosen stabilization, the error e_h is estimated either in the standard norm or the stabilization semi-norm leading to different orders of convergence in the spatial parameter h. This will be discussed in detail in the corresponding examples below.

Proof of Theorem 3.4. We insert the projected exact solutions into the discretized equations (3.2) to obtain

$$\begin{aligned}
&p(\partial_t J_h x, y_h) + s_h(J_h x, y_h) + \widetilde{b}_h(\widetilde{J}_h \theta, y_h) - p(f_h, y_h) \\
&\qquad + \widetilde{p}(\partial_t \widetilde{J}_h \theta, \varphi_h) + \widetilde{s}(\widetilde{J}_h \theta, \varphi_h) - \widetilde{b}_h(\varphi_h, J_h x) - \widetilde{p}(g_h, \varphi_h) \\
&= p(\partial_t x, y_h) + \Delta p(\partial_t x, y_h) + \widehat{s}(x, y_h) + \widehat{b}(\theta, y_h) + \Delta_{s,b}(x,\theta,y_h) - p(f, y_h) - \Delta f(y_h) \\
&\quad + \widetilde{p}(\partial_t \theta, \varphi_h) + \Delta \widetilde{p}(\partial_t \theta, \varphi_h) + \widetilde{s}(\theta, \varphi_h) - \widetilde{b}(\varphi_h, x) + \widetilde{\Delta}_{s,b}(x,\theta,\varphi_h) - \widetilde{p}(g, \varphi_h) - \Delta g(\varphi_h) \\
&= \Delta p(\partial_t x, y_h) + \Delta_{s,b}(x,\theta,y_h) - \Delta f(y_h) + \widetilde{p}(\partial_t \theta, \varphi_h) + \widetilde{\Delta}_{s,b}(x,\theta,\varphi_h) - \Delta g(\varphi_h),
\end{aligned}$$

where we used in the last step that (2.2) also holds when tested with discrete functions $(y_h,\varphi_h) \in X_h \times H_h$, see (2.3). Subtracting (3.2), we obtain the error equation

$$\begin{aligned}
&p(\partial_t e_h, y_h) + s_h(e_h, y_h) + \widetilde{b}_h(\epsilon_h, y_h) + \widetilde{p}(\partial_t \epsilon_h, \varphi_h) + \widetilde{s}(\epsilon_h, \varphi_h) - \widetilde{b}_h(\varphi_h, e_h) \\
&= \Delta p(\partial_t x, y_h) + \Delta_{s,b}(x,\theta,y_h) - \Delta f(y_h) + \widetilde{p}(\partial_t \theta, \varphi_h) + \widetilde{\Delta}_{s,b}(x,\theta,\varphi_h) - \Delta g(\varphi_h).
\end{aligned}$$

Testing with $(y_h,\varphi_h) = (e_h,\epsilon_h)$, using (3.3), integrating in time, and finally a weighted Gronwall argument yields the claim. □

4. Full discretization

Since we aim to apply a leapfrog-type method to the wave system, we need to exploit again the two-field structure of the problem and assume that also the discrete bilinear form s_h can be decomposed as

$$s_h^s(x_h, y_h) = s_{h,1}(x_{h,1}, y_{h,2}) - s_{h,2}(x_{h,2}, y_{h,1}),$$

and we have the representation

$$s_h^p(x_h, y_h) = s_h^{p,1}(x_{h,1}, y_{h,1}) + s_h^{p,2}(x_{h,2}, y_{h,2})$$

for the stabilization. Further, the coupling term is given by

$$\widetilde{b}_h(\theta_h, y_h) = b_h(\theta_h, y_{h,1}),$$

see (2.1). With this, we can formulate our problem equivalently as

$$p_1(\partial_t x_{h,1}, y_{h,1}) - s_{h,2}(x_{h,2}, y_{h,1}) = -b_h(\theta_h, y_{h,1}) + p_1(f_{h,1}, y_{h,1}) \tag{4.1a}$$

$$p_2(\partial_t x_{h,2}, y_{h,2}) + s_{h,1}(x_{h,1}, y_{h,2}) = 0 \tag{4.1b}$$

$$\widetilde{p}(\partial_t \theta_h, \varphi_h) + \widetilde{s}(\theta_h, \varphi_h) = b_h(\varphi_h, x_{h,1}) + \widetilde{p}(g_h, \varphi_h) \tag{4.1c}$$

or in the strong form as

$$\partial_t x_{h,1} - S_{h,2} x_{h,2} + S^p_{h,1} x_{h,1} = -B_h \theta_h + f_{h,1} \tag{4.2a}$$

$$\partial_t x_{h,2} + S_{h,1} x_{h,1} + S^p_{h,2} x_{h,2} = 0 \tag{4.2b}$$

$$\partial_t \theta_h + L_h \theta_h = B_h^* x_{h,1} + g_h, \tag{4.2c}$$

which is the starting point for our time integration scheme.

4.1. **Derivation of the method.** In the following, we denote the time step size as $\tau > 0$ and define the times $t_n = n\tau$, $n \geq 0$. In order to see the structural similarity of our fully discrete method, we formulate the system as a single first-order evolution equation with variable $\mathcal{U} = \big(x_1, x_2, \theta\big)$ in the form

$$\partial_t \mathcal{U}(t) + \boldsymbol{\mathcal{A}} \mathcal{U}(t) = \mathcal{F}(t), \qquad \boldsymbol{\mathcal{A}} = \begin{pmatrix} 0 & -S_2 & B \\ S_1 & 0 & 0 \\ -B^* & 0 & L \end{pmatrix}, \qquad \mathcal{F} = \begin{pmatrix} f_1 \\ 0 \\ g \end{pmatrix}. \tag{4.3}$$

Further, we introduce the fully discrete approximations and their collections

$$x^n_{h,1} \approx x_{h,1}(t_n), \quad x^n_{h,2} \approx x_{h,2}(t_n), \quad \theta^n_h \approx \theta_h(t_n), \quad \mathcal{U}^n_h = \big(x^n_{h,1}, x^n_{h,2}, \theta^n_h\big).$$

We derive our time stepping scheme in two steps. Assume for a moment that the field θ_h is known at all time steps. The well-known leapfrog scheme for the wave equation described by (4.2a) and (4.2b) in half-step formulation (staggerd) then reads

$$x^{n+1/2}_{h,1} = x^n_{h,1} + \frac{\tau}{2} S_{h,2} x^n_{h,2} - \frac{\tau}{2} S^p_{h,1} x^n_{h,1} - \frac{\tau}{2} B_h \theta^n_h + \frac{\tau}{2} f^n_{h,1}, \tag{4.4a}$$

$$x^{n+1}_{h,2} = x^n_{h,2} - \tau S_{h,1} x^{n+1/2}_{h,1} - \tau S^p_{h,2} x^n_{h,2}, \tag{4.4b}$$

$$x^{n+1}_{h,1} = x^{n+1/2}_{h,1} + \frac{\tau}{2} S_{h,2} x^{n+1}_{h,2} - \frac{\tau}{2} S^p_{h,1} x^n_{h,1} - \frac{\tau}{2} B_h \theta^{n+1}_h + \frac{\tau}{2} f^{n+1}_{h,1}. \tag{4.4c}$$

Here, $x^{n+1/2}_{h,1} \approx \frac{1}{2}\big(x^{n+1}_{h,1} + x^n_{h,1}\big)$ is a second order in τ approximation to the mean value. Since the stabilization terms break the Hamiltonian structure of the discrete wave equation, it is common practice to apply them in such a way that the scheme stays explicit. Note that (4.4a) and (4.4b) are explicitly computable from known values at time $t = t_n$. Step (4.4c), on the other hand, is not explicitly computable since it demands the yet unknown value θ^{n+1}_h. In hope to omit any CFL condition from the heat part, we introduce a Crank–Nicolson step for (4.2c), which reads

$$\theta^{n+1}_h = \theta^n_h - \frac{\tau}{2} L_h\big(\theta^{n+1}_h + \theta^n_h\big) + \frac{\tau}{2} B^*_h\big(x^{n+1}_{h,1} + x^n_{h,1}\big) + \frac{\tau}{2}\big(g^{n+1}_h + g^n_h\big). \tag{4.5}$$

The average of $x_{h,1}$ in (4.5) makes the coupling of (4.5) and (4.4c) implicit, which is undesired. Circumventing this, we replace the average with the already calculated

half-step $x_{h,1}^{n+1/2}$ and obtain the approximation

$$\theta_h^{n+1} \approx \theta_h^n - \frac{\tau}{2} L_h\big(\theta_h^{n+1} + \theta_h^n\big) + \tau B_h^* x_{h,1}^{n+1/2} + \frac{\tau}{2}\big(g_h^{n+1} + g_h^n\big). \tag{4.6}$$

Since the half-step is a second order in τ approximation of the average, we expect the scheme described by the coupling of (4.4) and (4.6) to keep its good properties and convergence rate.

Summarizing this, our proposed time stepping scheme reads

$$x_{h,1}^{n+1/2} = x_{h,1}^n + \frac{\tau}{2} S_{h,2} x_{h,2}^n - \frac{\tau}{2} S_{h,1}^p x_{h,1}^n - \frac{\tau}{2} B_h \theta_h^n + \frac{\tau}{2} f_{h,1}^n, \tag{4.7a}$$

$$x_{h,2}^{n+1} = x_{h,2}^n - \tau S_{h,1} x_{h,1}^{n+1/2} - \tau S_{h,2}^p x_{h,2}^n, \tag{4.7b}$$

$$\theta_h^{n+1} = \theta_h^n - \frac{\tau}{2} L_h\big(\theta_h^{n+1} + \theta_h^n\big) + \tau B_h^* x_{h,1}^{n+1/2} + \frac{\tau}{2}\big(g_h^{n+1} + g_h^n\big), \tag{4.7c}$$

$$x_{h,1}^{n+1} = x_{h,1}^{n+1/2} + \frac{\tau}{2} S_{h,2} x_{h,2}^{n+1} - \frac{\tau}{2} S_{h,1}^p x_{h,1}^n - \frac{\tau}{2} B_h \theta_h^{n+1} + \frac{\tau}{2} f_{h,1}^{n+1}. \tag{4.7d}$$

The rest of this manuscript is devoted to prove stability and convergence of the scheme, as well as to the demonstration of it to the different examples.

4.2. **Stability.** We prove stability by rewriting (4.7) as a perturbed evolution equation, deploying energy estimates and closing with a Gronwall-type argument. Let $\{\alpha_n\}_{n\geq 0} \subset \mathbb{R}^\ell$ be a series for given $\ell \geq 1$. We define the average and discrete derivative of the series as

$$\overline{\alpha}^{n+1} = \frac{\alpha^{n+1} + \alpha^n}{2}, \quad \partial_\tau \alpha^{n+1} = \frac{\alpha^{n+1} - \alpha^n}{\tau}, \qquad n \geq 0.$$

We derive the perturbed evolution equation of (4.7). Subtraction of (4.7d) from (4.7a) and rearranging gives

$$x_{h,1}^{n+1/2} = \overline{x}_{h,1}^{n+1} - \frac{\tau^2}{4} S_{h,2} \partial_\tau x_{h,2}^{n+1} + \frac{\tau^2}{4} B_h \partial_\tau \theta_h^{n+1} - \frac{\tau^2}{4} \partial_\tau f_{h,1}^{n+1}. \tag{4.8}$$

Addition of (4.7a) and (4.7d) on the other hand shows

$$\partial_\tau x_{h,1}^{n+1} - S_{h,2} \overline{x}_{h,2}^{n+1} + S_{h,1}^p x_{h,1}^n + B_h \overline{\theta}_h^{n+1} = \overline{f}_{h,1}^{n+1}. \tag{4.9}$$

Insertion of (4.8) in (4.7b) gives

$$\begin{aligned} &\partial_\tau x_{h,2}^{n+1} + S_{h,1} \overline{x}_{h,1}^{n+1} + S_{h,2}^p x_{h,2}^n \\ &\quad = \frac{\tau^2}{4} S_{h,1} S_{h,2} \partial_\tau x_{h,2}^{n+1} - \frac{\tau^2}{4} S_{h,1} B_h \partial_\tau \theta_h^{n+1} + \frac{\tau^2}{4} S_{h,1} \partial_\tau f_{h,1}^{n+1}. \end{aligned} \tag{4.10}$$

Again, insertion of (4.8) in (4.7c) shows

$$\begin{aligned} &\partial_\tau \theta_h^{n+1} + L_h \overline{\theta}_h^{n+1} - B_h^* \overline{x}_{h,1}^{n+1} \\ &\quad = \overline{g}_h^{n+1} - \frac{\tau^2}{4} B_h^* S_{h,2} \partial_\tau x_{h,2}^{n+1} + \frac{\tau^2}{4} B_h^* B_h \partial_\tau \theta_h^{n+1} - \frac{\tau^2}{4} B_h^* \partial_\tau f_{h,1}^{n+1}. \end{aligned} \tag{4.11}$$

Gathering (4.9), (4.10) and (4.11), we obtain the perturbed discrete evolution equation for the collection $\mathcal{U}_h^n = \big(x_{h,1}^n, x_{h,2}^n, \theta_h^n\big)$

$$\big(1 - \frac{\tau}{2}\boldsymbol{\mathcal{S}}_h - \frac{\tau^2}{4}\boldsymbol{\mathcal{D}}_h\big)\partial_\tau \mathcal{U}_h^{n+1} + \big(\boldsymbol{\mathcal{A}}_h + \boldsymbol{\mathcal{S}}_h\big)\overline{\mathcal{U}}_h^{n+1} = \overline{\mathcal{F}}_h^{n+1} - \frac{\tau^2}{4}\boldsymbol{\mathcal{G}}_h \partial_\tau f_{h,1}^{n+1}, \quad n \geq 0, \tag{4.12}$$

where $\mathcal{F}_h^n = \big(f_{h,1}^n, 0, g_h^n\big)$ and

$$\boldsymbol{\mathcal{A}}_h = \begin{pmatrix} 0 & -S_{h,2} & B_h \\ S_{h,1} & 0 & 0 \\ -B_h^* & 0 & L_h \end{pmatrix}, \quad \boldsymbol{\mathcal{S}}_h = \begin{pmatrix} S_{h,1}^p & 0 & 0 \\ 0 & S_{h,2}^p & 0 \\ 0 & 0 & 0 \end{pmatrix}, \tag{4.13}$$

$$\boldsymbol{\mathcal{D}}_h = \begin{pmatrix} 0 & 0 & 0 \\ 0 & S_{h,1}S_{h,2} & -S_{h,1}B_h \\ 0 & -B_h^*S_{h,2} & B_h^*B_h \end{pmatrix}, \quad \boldsymbol{\mathcal{G}}_h = \begin{pmatrix} 0 \\ -S_{h,1} \\ B_h^* \end{pmatrix}, \tag{4.14}$$

and the application of $\boldsymbol{\mathcal{G}}_h$ is understood component wise.

Lemma 4.1. *Let Assumptions 2.1 and 3.2 hold.*
(a) The operator $\boldsymbol{\mathcal{A}}_h : Y_h \times V_h \to Y_h \times V_h$ is accretive, i.e.,

$$\langle \boldsymbol{\mathcal{A}}_h \mathcal{V}_h, \mathcal{V}_h \rangle_{p\times\widetilde{p}} \geq 0, \quad \forall \mathcal{V}_h \in Y_h \times V_h.$$

(b) Let $\mathcal{V}_h, \mathcal{W}_h \in Y_h \times V_h$. If the last component of $\mathcal{V}_h$ or $\mathcal{W}_h$ is zero, then

$$\langle \boldsymbol{\mathcal{A}}_h \mathcal{V}_h, \mathcal{W}_h \rangle_{p\times\widetilde{p}} = -\langle \mathcal{V}_h, \boldsymbol{\mathcal{A}}_h \mathcal{W}_h \rangle_{p\times\widetilde{p}}. \tag{4.15}$$

Proof. (a) Let $\mathcal{V}_h = \big(y_{h,1}, y_{h,2}, \varphi_h\big) \in Y_h \times V_h$. By definition, we obtain

$$\begin{aligned}
\langle \boldsymbol{\mathcal{A}}_h \mathcal{V}_h, \mathcal{V}_h \rangle_{p\times\widetilde{p}} &= p_1(-S_{h,2}y_{h,2}, y_{h,1}) + p_1(B_h\varphi_h, y_{h,1}) + p_2(S_{h,1}y_{h,1}, y_{h,2}) \\
&\qquad + \widetilde{p}(-B_h^* y_{h,1}, \varphi_h) + \widetilde{p}(L_h\varphi_h, \varphi_h) \\
&= s_{h,1}(y_{h,1}, y_{h,2}) - s_{h,2}(y_{h,2}, y_{h,1}) + \widetilde{s}(\varphi_h, \varphi_h) \\
&\qquad + b_h(\varphi_h, y_{h,1}) - b_h(\varphi_h, y_{h,1}) \\
&= s_h^s(y_h, y_h) + \widetilde{s}(\varphi_h, \varphi_h) \\
&= \widetilde{s}(\varphi_h, \varphi_h) \\
&\geq 0,
\end{aligned}$$

where $y_h = (y_{h,1}, y_{h,2})$ and Assumption 2.1 and 3.2 were used in the last inequality. The second claim (b) is a direct consequence of Assumption 3.2. □

In the following, we frequently use the discrete version of differentiation of a square norm. Let $\{\alpha^n\}_{n\geq 0} \subset \mathbb{R}^\ell$, for $\ell \geq 1$, and $|\cdot|_\ell$ denote the Euclidean norm. It holds that

$$\partial_\tau \frac{1}{2}|\alpha^n|_\ell^2 = \frac{1}{2\tau}\big(|\alpha^{n+1}|_\ell^2 - |\alpha^n|_\ell^2\big) = \partial_\tau \alpha^n \cdot \overline{\alpha}^n. \tag{4.16}$$

We obtain the following equality for the perturbation.

Lemma 4.2. *Let $\{\mathcal{V}_h^n\}_{n\geq 0} \subset Y_h \times V_h$. It holds for $n \geq 0$*

$$\frac{\tau^2}{4}\langle \boldsymbol{\mathcal{D}}_h \partial_\tau \mathcal{V}_h^{n+1}, \overline{\mathcal{V}}_h^{n+1} \rangle_{p\times\widetilde{p}} = \frac{\tau}{8}\Big(\|S_{h,2}x_{h,2}^{n+1} - B_h x_{h,2}^{n+1}\|_{p_1}^2 - \|S_{h,2}x_{h,2}^{n} - B_h x_{h,2}^{n}\|_{p_1}^2\Big).$$

Proof. We use the definition in (4.14), and compute

$$\begin{aligned}\langle \boldsymbol{\mathcal{D}}_h \partial_\tau \mathcal{V}_h^{n+1}, \overline{\mathcal{V}}_h^{n+1}\rangle_{p\times\widetilde{p}} &= p_2(S_{h,1}S_{h,2}\partial_\tau x_{h,2}^{n+1}, \overline{x}_{h,2}^{n+1}) - p_2(S_{h,1}B_h\partial_\tau\theta_h^{n+1}, \overline{\theta}_h^{n+1})\\ &\quad - \widetilde{p}(B_h^* S_{h,2}\partial_\tau x_{h,2}^{n+1}, \overline{\theta}_h^{n+1}) + \widetilde{p}(B_h^* B_h\partial_\tau\theta_h^{n+1}, \overline{\theta}_h^{n+1})\\ &= p_1(S_{h,2}\partial_\tau x_{h,2}^{n+1}, S_{h,2}\overline{x}_{h,2}^{n+1}) - p_1(B_h\partial_\tau\theta_h^{n+1}, S_{h,2}\overline{x}_{h,2}^{n+1})\\ &\quad - p_1(S_{h,2}\partial_\tau x_{h,2}^{n+1}, B_h\overline{\theta}_h^{n+1}) + p_1(B_h\partial_\tau\theta_h^{n+1}, B_h\overline{\theta}_h^{n+1})\\ &= p_1(S_{h,2}\partial_\tau x_{h,2}^{n+1} - B_h\partial_\tau\theta_h^{n+1}, S_{h,2}\overline{x}_{h,2}^{n+1} - B_h\overline{\theta}_h^{n+1})\\ &= \frac{1}{2\tau}\Big(\|S_{h,2}x_{h,2}^{n+1} - B_h\theta_h^{n+1}\|_{p_1}^2 - \|S_{h,2}x_{h,2}^{n} - B_h\theta_h^{n}\|_{p_1}^2\Big),\end{aligned}$$

where we employed (4.16) in the last step. □

This allows us to conclude the following energy inequality for some general right-hand side. Later on, this estimate will also be used for the error recursion and the defects as right-hand sides.

Lemma 4.3. *Let $K_h^{n+1} = (k_{h,1}^{n+1}, k_{h,2}^{n+1}, \kappa_h^{n+1}) \in X_h \times H_h$ for $n \geq 0$. Then, the recursion*

$$\big(1 - \frac{\tau}{2}\boldsymbol{\mathcal{S}}_h - \frac{\tau^2}{4}\boldsymbol{\mathcal{D}}_h\big)\partial_\tau \mathcal{U}_h^{n+1} + \big(\boldsymbol{\mathcal{A}}_h + \boldsymbol{\mathcal{S}}_h\big)\overline{\mathcal{U}}_h^{n+1} = K_h^{n+1}, \quad n \geq 0, \tag{4.17}$$

satisfies for $n \geq 0$ the estimate

$$\begin{aligned}&\|\mathcal{U}_h^{n+1}\|_{p\times\widetilde{p}}^2 - \frac{\tau}{2}|x_h^{n+1}|_{s_h^p}^2 - \frac{\tau^2}{4}\|S_{h,2}x_{h,2}^{n+1} - B_h x_{h,2}^{n+1}\|_{p_1}^2 + 2\tau|\overline{x_h}^{n+1}|_{s_h^p}^2\\ &\quad\leq \|\mathcal{U}_h^{n}\|_{p\times\widetilde{p}}^2 - \frac{\tau}{2}|x_h^{n}|_{s_h^p}^2 - \frac{\tau^2}{4}\|S_{h,2}x_{h,2}^{n} - B_h x_{h,2}^{n}\|_{p_1}^2 + 2\tau\langle K_h^{n+1}, \overline{\mathcal{U}}_h^{n+1}\rangle_{p\times\widetilde{p}}.\end{aligned} \tag{4.18}$$

Proof. We test (4.17) with $\overline{\mathcal{U}}_h^{n+1}$ and obtain for the first term and (4.16) that

$$\langle \partial_\tau \mathcal{U}_h^{n+1}, \overline{\mathcal{U}}_h^{n+1}\rangle_{p\times\widetilde{p}} = \frac{1}{2\tau}\Big(\|\mathcal{U}_h^{n+1}\|_{p\times\widetilde{p}}^2 - \|\mathcal{U}_h^{n}\|_{p\times\widetilde{p}}^2\Big).$$

For the second term we obtain again with (4.16)

$$\frac{\tau}{2}\langle \boldsymbol{\mathcal{S}}_h\partial_\tau \mathcal{U}_h^{n+1}, \overline{\mathcal{U}}_h^{n+1}\rangle_{p\times\widetilde{p}} = \frac{1}{4}|x_h^{n+1}|_{s_h^p}^2 - \frac{1}{4}|x_h^{n}|_{s_h^p}^2.$$

The third term is already controlled by Lemma 4.2, thus it remains to estimate the fourth term. With Lemma 4.1, we see that

$$|\overline{x_h}^{n+1}|_{s_h^p}^2 = \langle \boldsymbol{\mathcal{S}}_h\overline{\mathcal{U}}_h^{n+1}, \overline{\mathcal{U}}_h^{n+1}\rangle_{p\times\widetilde{p}} \leq \langle \big(\boldsymbol{\mathcal{A}}_h + \boldsymbol{\mathcal{S}}_h\big)\overline{\mathcal{U}}_h^{n+1}, \overline{\mathcal{U}}_h^{n+1}\rangle_{p\times\widetilde{p}}$$

Gathering all estimates and multiplication with 2τ proves the claim. □

We proceed proving stability under the following CFL condition.

Assumption 4.4. Given $\eta \in (0,1)$ there exists $\tau_{\mathrm{CFL}} > 0$ such that for all $\tau \leq \tau_{\mathrm{CFL}}$ and $\mathcal{U}_h = (x_h, \theta_h) \in Y_h \times V_h$ it holds

$$\frac{\tau^2}{2}\|S_{h,2}x_{h,2}\|_{p_1}^2 + \frac{\tau^2}{2}\|B_h\theta_h\|_{p_1}^2 + \tau|x_h|_{s_h^p}^2 \leq \eta\|\mathcal{U}_h\|_{p\times\widetilde{p}}^2. \tag{4.19}$$

We note that the assumption directly implies the bound

$$\tau\|\boldsymbol{\mathcal{S}}_h\| \leq \eta, \tag{4.20}$$

which is used throughout the error analysis.

Remark 4.5. Note that we expect the first two norms in (4.19) to scale inverse with the minimal mesh size $h_{\min}$, and the third with $h_{\min}^{1/2}$. Thus, we consider a step-size restriction $\tau \approx h_{\min}$. Usually, the stabilization depends on a user-given parameter set. The second norm in (4.19) is expected to scale inverse with these parameters. Hence, the CFL condition becomes slightly worse with stronger stabilization.

Theorem 4.6. *Let Assumption 4.4 hold. For the recursion* (4.17) *it holds*

$$\begin{aligned}(1-\eta)\|\mathcal{U}_h^{n+1}\|_{p\times\widetilde{p}}^2 + \frac{\tau}{2}\sum_{\ell=0}^{n}|x_h^{\ell+1}+x_h^{\ell}|_{s_h^p}^2 \\ \leq e^{3/2}\|\mathcal{U}_h^0\|_{p\times\widetilde{p}}^2 + \frac{e^{3/2}T}{(1-\eta)}\tau\sum_{l=0}^{n+1}\|K_h^{\ell+1}\|_{p\times\widetilde{p}}^2.\end{aligned}$$

Proof. Summation in (4.18) shows

$$\begin{aligned}\|\mathcal{U}_h^{n+1}\|_{p\times\widetilde{p}}^2 + 2\tau\sum_{\ell=0}^{n}|\overline{x_h}^{\ell+1}|_{s_h^p}^2 \leq \|\mathcal{U}_h^0\|_{p\times\widetilde{p}}^2 + \frac{\tau}{2}|x_h^{n+1}|_{s_h^p}^2 \\ + \frac{\tau^2}{4}\|S_{h,2}x_{h,2}^{n+1} - B_h x_{h,2}^{n+1}\|_{p_1}^2 + 2\tau\sum_{\ell=0}^{n}\langle K_h^{\ell+1}, \overline{\mathcal{U}}_h^{\ell+1}\rangle_{p\times\widetilde{p}}.\end{aligned}$$

With (4.19), we conclude that

$$(1-\eta)\|\mathcal{U}_h^{n+1}\|_{p\times\widetilde{p}}^2 + 2\tau\sum_{\ell=0}^{n}|\overline{x_h}^{\ell+1}|_{s_h^p}^2 \leq \|\mathcal{U}_h^0\|_{p\times\widetilde{p}}^2 + 2\tau\sum_{\ell=0}^{n}\langle K_h^{\ell+1}, \overline{\mathcal{U}}_h^{\ell+1}\rangle_{p\times\widetilde{p}}.$$

We estimate the remaining product with Young and obtain

$$\begin{aligned}2\tau\sum_{\ell=0}^{n}\langle K_h^{\ell+1}, \overline{\mathcal{U}}_h^{\ell+1}\rangle_{p\times\widetilde{p}} \leq \frac{(1-\eta)}{2T}\frac{\tau}{2}\sum_{\ell=0}^{n}\Big(\|\mathcal{U}_h^{\ell+1}\|_{p\times\widetilde{p}}^2 + \|\mathcal{U}_h^{\ell}\|_{p\times\widetilde{p}}^2\Big) \\ + \frac{T\tau}{(1-\eta)}\sum_{\ell=0}^{n}\|K_h^{\ell+1}\|_{p\times\widetilde{p}}^2.\end{aligned}$$

Therefore, we see that

$$\begin{aligned}(1-\eta)\|\mathcal{U}_h^{n+1}\|_{p\times\widetilde{p}}^2 + \frac{\tau}{2}\sum_{\ell=0}^{n}|x_h^{\ell+1}+x_h^{\ell}|_{s_h^p}^2 \\ \leq \|\mathcal{U}_h^0\|_{p\times\widetilde{p}}^2 + \frac{(1-\eta)}{2T}\frac{\tau}{2}\sum_{\ell=0}^{n}\Big(\|\mathcal{U}_h^{\ell+1}\|_{p\times\widetilde{p}}^2 + \|\mathcal{U}_h^{\ell}\|_{p\times\widetilde{p}}^2\Big) + \frac{T\tau}{(1-\eta)}\sum_{\ell=0}^{n}\|K_h^{\ell+1}\|_{p\times\widetilde{p}}^2.\end{aligned}$$

Finally, the application of a discrete Gronwall estimate [Emm99, Proposition 4.1] proves the claim. □

Using the CFL condition (4.19) and the special structure of the right-hand side, we may conclude the following stability estimate.

Corollary 4.7. *Let Assumption 4.4 hold. Then, the time integration scheme* (4.7) *is stable and*

$$\begin{aligned}(1-\eta)\|\mathcal{U}_h^{n+1}\|_{p\times\widetilde{p}}^2 + \frac{\tau}{2}\sum_{\ell=0}^{n}|x_h^{\ell+1}+x_h^{\ell}|_{s_h^p}^2 \\ \leq e^{3/2}\|\mathcal{U}_h^0\|_{p\times\widetilde{p}}^2 + \frac{2e^{3/2}T}{(1-\eta)}\tau\sum_{l=0}^{n+1}(1+\eta)\|f_{h,1}^{\ell}\|_{p_1}^2 + \|g_h^{\ell}\|_{\widetilde{p}}^2.\end{aligned}$$

Proof. First we note that the CFL condition (4.19) on $S_{h,2}$ implies the same condition on $S_{h,1}$ by adjointness. It holds that

$$\begin{aligned}\frac{\tau}{\sqrt{2}}p_2(S_1x_{h,1},x_{h,2}) &= \frac{\tau}{\sqrt{2}}p_1(x_{h,1},S_{h,2}x_{h,2}) \\ &\leq \|x_{h,1}\|_{p_1}\frac{\tau}{\sqrt{2}}\|S_{h,2}x_{h,2}\|_{p_1} \\ &\leq \eta^{1/2}\|x_{h,1}\|_{p_1}\|\mathcal{U}_h\|_{p\times\widetilde{p}},\end{aligned}$$

which implies that $\tau^2\|S_{h,1}x_{h,1}\|_{p_2}^2 \leq 4\eta\|\mathcal{U}_h\|_{p\times\widetilde{p}}$. Thus, we obtain

$$\begin{aligned}\frac{\tau^4}{16}\|\boldsymbol{\mathcal{G}}_h\partial_\tau f_{h,1}^{n+1}\|_{p\times\widetilde{p}}^2 &= \frac{\tau^4}{16}\|S_{h,1}\partial_\tau f_{h,1}^{n+1}\|_{p_2}^2 + \frac{\tau^4}{16}\|B_h^*\partial_\tau f_{h,1}^{n+1}\|_{\widetilde{p}}^2 \\ &\leq \eta\frac{\tau^2 1}{4}\|\partial_\tau f_{h,1}^{n+1}\|_{p_1}^2 \\ &\leq \eta\frac{1}{2}\big(\|f_{h,1}^{n+1}\|_{p_1}^2 + \|f_{h,1}^{n}\|_{p_1}^2\big).\end{aligned}$$

Furthermore, we see that

$$\|\overline{\mathcal{F}}_h^{n+1}\|_{p\times\widetilde{p}}^2 \leq \|f_{h,1}^{n+1}\|_{p_1}^2 + \|f_{h,1}^{n}\|_{p_1}^2 + \|g_{h,1}^{n+1}\|_{\widetilde{p}}^2 + \|g_{h,1}^{n}\|_{\widetilde{p}}^2.$$

The claim now follows with $K_h^{n+1} = \overline{\mathcal{F}}_h^{n+1} + \boldsymbol{\mathcal{G}}_h\partial_\tau f_{h,1}^{n+1}$ and Theorem 4.6. □

4.3. **Error analysis.** In the following, we derive an error recursion in the form of (4.12) in order to exploit the derived stability estimates, where the right-hand side will be given by the defects. Thus, we derive the defects in the first step. We begin with the defect of the Crank–Nicolson method and treat the rest as a perturbation. We introduce the full projections in the collection variable

$$\mathbf{P}_h = (P_h, \widetilde{P}_h), \qquad \mathbf{J}_h = (J_h, \widetilde{J}_h),$$

and abbreviate $\mathcal{U}^n = \mathcal{U}(t_n)$. The defect D_{CN}^{n+1} is given as

$$\partial_\tau\mathbf{J}_h\mathcal{U}^{n+1} + \boldsymbol{\mathcal{A}}_h\mathbf{J}_h\overline{\mathcal{U}}^{n+1} + \boldsymbol{\mathcal{S}}_h\mathbf{J}_h\mathcal{U}^n = \overline{\mathcal{F}}_h^{n+1} + D_{\mathrm{CN}}^{n+1}.$$

Inserting the exact solution (4.3), the defect has the form

$$\begin{aligned}D_{\mathrm{CN}}^{n+1} = \mathbf{P}_hD_{\mathrm{tr}}^{n+1} + \boldsymbol{\mathcal{S}}_h\mathbf{J}_h\mathcal{U}^n + \partial_\tau(\mathbf{J}_h-\mathbf{P}_h)\mathcal{U}^{n+1} \\ + (\boldsymbol{\mathcal{A}}_h\mathbf{J}_h - \mathbf{P}_h\boldsymbol{\mathcal{A}})\overline{\mathcal{U}}^{n+1} + \overline{\mathcal{F}}_h^{n+1} - \overline{\widehat{\mathcal{F}}}_h^{n+1},\end{aligned}$$

where D_{tr}^{n+1} is given by

$$D_{\mathrm{tr}}^{n+1} = \tau^2\int_0^1 k_{\mathrm{tr}}(\sigma)\,\partial_t^3\mathcal{U}(t_n+\tau\sigma)\,d\sigma$$

for some bounded Peano kernel k_{tr}. In the following Lemma, we provide estimates of this defect, noting that all the terms defined in (3.4) appear again.

Lemma 4.8. *Let $\mathcal{V}_h = \big(y_{h,1}, y_{h,2}, \varphi_h\big) \in Y_h \times V_h$. The defect can be decomposed into*

$$\langle D_{CN}^{n+1}, \mathcal{V}_h\rangle_{p\times\widetilde{p}} = \langle \widetilde{D}_{CN}^{n+1}, \mathcal{V}_h\rangle_{p\times\widetilde{p}} + \Delta_{s,b}(\overline{x}^{n+1}, \overline{\theta}^{n+1}, y_h),$$

where the first part satisfies the estimate

$$\begin{aligned}\|\widetilde{D}_{CN}^{n+1}\|_{X_h^*\times H_h^*} \leq \tau^2\|\partial_t^3\mathcal{U}\|_{X\times H} + (1+\frac{\eta}{2})\|\Delta p(\partial_\tau x^{n+1})\|_{X_h^*} + \|\Delta\widetilde{p}(\partial_\tau\theta^{n+1})\|_{H_h^*}\\ + \|\widetilde{\Delta}_{s,b}(\overline{x}^{n+1}, \overline{\theta}^{n+1})\|_{H_h^*} + \|\Delta\overline{f}^{n+1}\|_{X_h^*}^2 + \|\Delta\overline{g}^{n+1}\|_{H_h^*}^2,\end{aligned}$$

without additional constants.

Proof. The first part of the estimate follows directly from the boundedness of the Peano kernel. Further, we note that for the discrete test function $\mathcal{V}_h$, we have

$$\langle\partial_\tau(\mathbf{J}_h - \mathbf{P}_h)\mathcal{U}^{n+1}, \mathcal{V}_h\rangle_{p\times\widetilde{p}} = \Delta p(\partial_\tau x^{n+1}, y_h) + \Delta\widetilde{p}(\partial_\tau\theta^{n+1}, \varphi_h),$$

and taking into account the manipulation

$$\boldsymbol{\mathcal{S}}_h\mathbf{J}_h\mathcal{U}^n + (\boldsymbol{\mathcal{A}}_h\mathbf{J}_h - \mathbf{P}_h\boldsymbol{\mathcal{A}})\overline{\mathcal{U}}^{n+1} = -\frac{\tau}{2}\boldsymbol{\mathcal{S}}_h\mathbf{J}_h\partial_\tau\mathcal{U}^{n+1} + ((\boldsymbol{\mathcal{A}}_h + \boldsymbol{\mathcal{S}}_h)\mathbf{J}_h - \mathbf{P}_h\boldsymbol{\mathcal{A}})\overline{\mathcal{U}}^{n+1},$$

we recover by a straightforward calculation

$$\langle((\boldsymbol{\mathcal{A}}_h + \boldsymbol{\mathcal{S}}_h)\mathbf{J}_h - \mathbf{P}_h\boldsymbol{\mathcal{A}})\overline{\mathcal{U}}^{n+1}, \mathcal{V}_h\rangle_{p\times\widetilde{p}} = \Delta_{s,b}(\overline{x}^{n+1}, \overline{\theta}^{n+1}, y_h) + \widetilde{\Delta}_{s,b}(\overline{x}^{n+1}, \overline{\theta}^{n+1}, \varphi_h).$$

Similarly, the right-hand side terms are treated as

$$\langle\overline{\mathcal{F}}_h^{n+1} - \overline{\widehat{\mathcal{F}}}_h^{n+1}, \mathcal{V}_h\rangle_{p\times\widetilde{p}} = \Delta\overline{f}^{n+1}(y_h) + \Delta\overline{g}^{n+1}(\varphi_h).$$

It remains to consider the stabilization term. We exploit that by Assumption 3.2 the exact solution vanishes under the stabilization operator, and obtain, using the CFL condition (4.20),

$$\|\frac{\tau}{2}\boldsymbol{\mathcal{S}}_h\mathbf{J}_h\partial_\tau\mathcal{U}^{n+1}\|_{X_h^*\times H_h^*} = \|\frac{\tau}{2}\boldsymbol{\mathcal{S}}_h(I-\mathbf{J}_h)\partial_\tau\mathcal{U}^{n+1}\|_{X_h^*\times H_h^*} = \frac{\eta}{2}\|\Delta p(\partial_\tau x^{n+1})\|_{X_h^*},$$

since the stabilization operator acts on the wave part only. □

Turning now to the full defect, we define

$$\begin{aligned}&\partial_\tau\mathbf{J}_h\mathcal{U}^{n+1} + \boldsymbol{\mathcal{A}}_h\mathbf{J}_h\overline{\mathcal{U}}^{n+1} + \boldsymbol{\mathcal{S}}_h\mathbf{J}_h\mathcal{U}^n\\ &= \overline{\mathcal{F}}_h^{n+1} + \frac{\tau^2}{4}\boldsymbol{\mathcal{D}}_h\partial_\tau\mathbf{J}_h\mathcal{U}^{n+1} - \frac{\tau^2}{4}\boldsymbol{\mathcal{G}}_h\partial_\tau f_{h,1}^{n+1} + D_{\mathrm{CN}}^{n+1} + D_{\mathrm{CNLF}}^{n+1},\end{aligned}$$

and thus we obtain the representation

$$D_{\mathrm{CNLF}}^{n+1} = -\frac{\tau^2}{4}\boldsymbol{\mathcal{D}}_h\partial_\tau\mathbf{J}_h\mathcal{U}^{n+1} + \frac{\tau^2}{4}\boldsymbol{\mathcal{G}}_h\partial_\tau f_{h,1}^{n+1},$$

which we study in more detail in the next lemma.

Lemma 4.9. *The defect D_{CNLF}^{n+1} can be factorized as*

$$D_{CNLF}^{n+1} = \frac{\tau^2}{4}\boldsymbol{\mathcal{A}}_h\partial_\tau\widetilde{D}^{n+1}, \quad \widetilde{D}^{n+1} = \begin{pmatrix} d^{n+1} - P_h^1\partial_t x_1^{n+1} \\ 0 \\ 0 \end{pmatrix},$$

with

$$d^{n+1} = (S_{h,2}J_h^1 - P_h^1S_2)x_2^{n+1} - (B_h\widetilde{J}_h - P_h^1B)\theta^{n+1} + f_{h,1}^{n+1} - P_h^1f_1^{n+1}f.$$

Further, we have the estimates for $k = 1, 2$

$$\begin{aligned}\tau^2\|\partial_\tau^k \widetilde{D}^{n+1}\|_{X_h^*} &\le \tau^2\big(\|\Delta_{s,b}^s(\partial_\tau^{k+1}x^{n+1}, \partial_\tau^{k+1}\theta^{n+1})\|_{X_h^*} \\ &\qquad + \|\Delta\partial_\tau^{k+1}f^{n+1}\|_{X_h^*} + \|\partial_t^{k+2}x_1^{n+1}\|_{S_{h,1}^*}\big),\\ \tau^2\|\boldsymbol{\mathcal{S}}_h^{1/2}\partial_\tau\widetilde{D}^{n+1}\|_{X_h^*} &\le \eta\tau^{3/2}\big(\|\Delta_{s,b}^s(\partial_\tau^2 x^{n+1}, \partial_\tau^2\theta^{n+1})\|_{X_h^*} \\ &\qquad + \|\Delta\partial_\tau^2 f^{n+1}\|_{X_h^*} + \|\Delta p(\partial_\tau^2\partial_t x^{n+1})\|_{X_h^*}\big),\end{aligned}$$

with constant independent of h *and* τ*, and* $\Delta_{s,b}^s$ *is defined as* $\Delta_{s,b}$ *in* (3.4b) *without the stabilization terms.*

Proof. For clarity, we omit all explicit time indices on the solution at time t_{n+1}. Writing the defect in its components, we observe

$$\boldsymbol{\mathcal{D}}_h\mathbf{J}_h\mathcal{U} = \begin{pmatrix} 0 \\ S_{h,1}(S_{h,2}J_h^1 x_2 - B_h\widetilde{J}_h\theta) \\ -B_h^*(S_{h,2}J_h^1 x_2 - B_h\widetilde{J}_h\theta)\end{pmatrix} = -\boldsymbol{\mathcal{G}}_h(S_{h,2}J_h^1 x_2 - B_h\widetilde{J}_h\theta)$$

as well as

$$\boldsymbol{\mathcal{G}}_h x_1 = -\boldsymbol{\mathcal{A}}_h\begin{pmatrix} x_1 \\ 0 \\ 0\end{pmatrix}.$$

In particular, this gives the proposed structure, and we have to estimate d^{n+1} and its discrete derivatives. First, we expand by using $-\partial_t x_1 = -S_2 x_2 + B\theta - f_1$

$$\begin{aligned}d - P_h^1\partial_t x_1 &= S_{h,2}J_h^1 x_2 - B_h\widetilde{J}_h\theta + f_{h,1}^{n+1} + P_h^1(-S_2x_2 + B\theta - f_1)\\ &= (S_{h,2}J_h^1 - P_h^1 S_2)x_2 - (B_h\widetilde{J}_h - P_h^1 B)\theta + f_{h,1}^{n+1} - P_h^1 f_1.\end{aligned}$$

We take the inner product with a discrete function $y_{h,1}$ to see

$$\begin{aligned}p_1(d - \partial_t x_1, y_{h,1}) &= p_1((S_{h,2}J_h^1 - P_h^1S_2)x_2 - (B_h\widetilde{J}_h - P_h^1B)\theta + f_{h,1}^{n+1} - P_h^1 f_1, y_{h,1})\\ &= s_{h,2}(J_h^1 x_2, y_{h,1}) - s_2(x_2, y_{h,1}) - b_h(\widetilde{J}_h\theta, y_{h,1}) + b(\theta, y_{h,1})\\ &\quad + p_1(f_{h,1}^{n+1} - f_1, y_{h,1})\\ &= \Delta_{s,b}^s(x, \theta, (y_{h,1}, 0)) + \Delta f(y_h),\end{aligned}$$

and we can directly deduce the first bound. For the second estimate, we again exploit that $\partial_t x_1$ vanishes under the stabilization operator, and thus we have

$$S_{h,1}^p P_h^1\partial_t x_1 = S_{h,1}^p(P_h^1 - I)\partial_t x_1,$$

and the CFL condition (4.20) gives the second estimate. □

Finally, we can define the discrete error $\mathcal{E}_h^n = \big(e_h^n, \epsilon_h^n\big) = \mathbf{J}_h\mathcal{U}^n - \mathcal{U}_h^n$ and obtain by subtraction of the above representation from the numerical method

$$(1 - \frac{\tau}{2}\boldsymbol{\mathcal{S}}_h - \frac{\tau^2}{4}\boldsymbol{\mathcal{D}}_h)\partial_\tau\mathcal{E}_h^{n+1} + \big(\boldsymbol{\mathcal{A}}_h + \boldsymbol{\mathcal{S}}_h\big)\overline{\mathcal{E}}_h^{n+1} = D_{\mathrm{CN}}^{n+1} + \frac{\tau^2}{4}\boldsymbol{\mathcal{A}}_h\partial_\tau\widetilde{D}^{n+1},$$

where we used the same identity as in the proof of Lemma 4.3. These preparations now allow us to deduce our second main result. We note that the limit $\tau \to 0$ formally recovers the statement of Theorem 3.4.

Theorem 4.10. *Let $x \in C^1([0,T],Y)$ and $\theta \in C^1([0,T],V)$ be the solution of (2.2), which satisfies $(x,\theta) \in C^1([0,T],\mathcal{Z})$ and $\mathcal{U} \in C^4([0,T],X\times H)$, and (x_h^n,θ_h^n) the solution of (4.4). Further, let Assumptions 2.1, 3.2, 3.3, and 4.4 hold true. Then, the fully discrete errors satisfy*

$$
\begin{aligned}
&\|e_h^{n+1}\|_{X_h}^2 + \|\epsilon_h^{n+1}\|_{H_h}^2 + \frac{\tau}{2}\sum_{\ell=0}^{n} |e_h^\ell + e_h^{\ell+1}|_{s_h^p}^2 \\
&\quad\lesssim \|e_h^0\|_{X_h}^2 + \|\epsilon_h^0\|_{H_h}^2 + C(\mathcal{U})\tau^4 \\
&\qquad + \tau\sum_{\ell=0}^{n} \|\Delta p(\partial_\tau x^{\ell+1})\|_{X_h^*}^2 + \|\Delta\widetilde{p}(\partial_\tau\theta^{\ell+1})\|_{H_h^*}^2 + \|\Delta\overline{f}^{\ell+1}\|_{X_h^*}^2 + \|\Delta\overline{g}^{\ell+1}\|_{H_h^*}^2, \\
&\qquad + \tau\sum_{\ell=0}^{n} \|\widetilde{\Delta}_{s,b}(x^{\ell+1},\theta^{\ell+1})\|_{H_h^*}^2 + |\Delta_{s,b}(\overline{x}^{\ell+1},\overline{\theta}^{\ell+1},\overline{e_h}^{\ell+1})| \\
&\qquad + \tau\sum_{\ell=0}^{n} \tau^4\big(\|\Delta_{s,b}^s(\partial_\tau^3 x^{\ell+1},\partial_\tau^3\theta^{\ell+1})\|_{X_h^*}^2 + \|\Delta\partial_\tau^3 f^{\ell+1}\|_{X_h^*} + \|\partial_t^4 x_1^{n+1}\|_{S_{h,1}^*}\big) \\
&\qquad + \tau\sum_{\ell=0}^{n} \tau^3\big(\|\Delta_{s,b}^s(\partial_\tau^2 x^{\ell+1},\partial_\tau^2\theta^{\ell+1})\|_{X_h^*}^2 + \|\Delta p(\partial_\tau^2\partial_t x^{\ell+1})\|_{X_h^*}^2\big)
\end{aligned}
$$

with constants independent of h and τ.

Proof. Using Lemma 4.3 and summing for $\ell = 0,\dots,n$, it remains to estimate

$$
2\tau\sum_{\ell=0}^{n}\langle K_h^{\ell+1},\overline{\mathcal{E}}_h^{\ell+1}\rangle_{p\times\widetilde{p}}, \quad \text{with } K_h^{\ell+1} = D_{\mathrm{CN}}^{\ell+1} + \frac{\tau^2}{4}\boldsymbol{\mathcal{A}}_h\partial_\tau\widetilde{D}^{\ell+1}.
$$

We can estimate as in Lemma 4.3, but have to take care of the latter term

$$
2\tau\sum_{\ell=0}^{n}\frac{\tau^2}{4}\langle\boldsymbol{\mathcal{A}}_h\partial_\tau\widetilde{D}^{\ell+1},\overline{\mathcal{E}}_h^{\ell+1}\rangle_{p\times\widetilde{p}}.
$$

Since $\widetilde{D}^{\ell+1}$ is zero in its last component, we use the skew-adjointness of $\boldsymbol{\mathcal{A}}_h$ in (4.15) and insert the error equation to obtain by Lemma 4.8

$$
\begin{aligned}
&-\langle\partial_\tau\widetilde{D}^{\ell+1},\boldsymbol{\mathcal{A}}_h\overline{\mathcal{E}}_h^{\ell+1}\rangle_{p\times\widetilde{p}} \\
&\quad= \langle\partial_\tau\widetilde{D}^{\ell+1},(I-\frac{\tau}{2}\boldsymbol{\mathcal{S}}_h-\frac{\tau^2}{4}\boldsymbol{\mathcal{D}}_h)\partial_\tau\mathcal{E}_h^{\ell+1} - \boldsymbol{\mathcal{S}}_h\overline{\mathcal{E}}_h^{\ell+1} + D_{\mathrm{CN}}^{\ell+1} + \boldsymbol{\mathcal{A}}_h\partial_\tau\widetilde{D}^{\ell+1}\rangle_{p\times\widetilde{p}} \\
&\quad= \langle\partial_\tau\widetilde{D}^{\ell+1},(I-\frac{\tau}{2}\boldsymbol{\mathcal{S}}_h-\frac{\tau^2}{4}\boldsymbol{\mathcal{D}}_h)\partial_\tau\mathcal{E}_h^{\ell+1}\rangle_{p\times\widetilde{p}} - \langle\boldsymbol{\mathcal{S}}_h^{1/2}\partial_\tau\widetilde{D}^{\ell+1},\boldsymbol{\mathcal{S}}_h^{1/2}\overline{\mathcal{E}}_h^{\ell+1}\rangle_{p\times\widetilde{p}} \\
&\qquad + \langle\partial_\tau\widetilde{D}^{\ell+1},\widetilde{D}_{\mathrm{CN}}^{\ell+1}\rangle_{p\times\widetilde{p}} + \Delta_{s,b}(\overline{x}^{\ell+1},\overline{\theta}^{\ell+1},\partial_\tau\widetilde{D}^{\ell+1}),
\end{aligned}
$$

where we again used the skew-adjointness for the cancellation of the $\boldsymbol{\mathcal{A}}_h \widetilde{D}^{\ell+1}$ term. For the first term, we apply summation by parts and conclude

$$\begin{aligned}
&\frac{\tau^2}{4}\tau\sum_{\ell=0}^{n}\langle\partial_\tau\widetilde{D}^{\ell+1},(I-\frac{\tau}{2}\boldsymbol{\mathcal{S}}_h-\frac{\tau^2}{4}\boldsymbol{\mathcal{D}}_h)\partial_\tau\mathcal{E}_h^{\ell+1}\rangle_{p\times\widetilde{p}}\\
&\quad=-\frac{\tau^2}{4}\tau\sum_{\ell=0}^{n}\langle\partial_\tau^2\widetilde{D}^{\ell+1},(I-\frac{\tau}{2}\boldsymbol{\mathcal{S}}_h-\frac{\tau^2}{4}\boldsymbol{\mathcal{D}}_h)\mathcal{E}_h^{\ell}\rangle_{p\times\widetilde{p}}\\
&\qquad+\frac{\tau^2}{4}\langle\partial_\tau\widetilde{D}^{n+1},(I-\frac{\tau}{2}\boldsymbol{\mathcal{S}}_h-\frac{\tau^2}{4}\boldsymbol{\mathcal{D}}_h)\mathcal{E}_h^{n+1}\rangle_{p\times\widetilde{p}}\\
&\qquad-\frac{\tau^2}{4}\langle\partial_\tau\widetilde{D}^{1},(I-\frac{\tau}{2}\boldsymbol{\mathcal{S}}_h-\frac{\tau^2}{4}\boldsymbol{\mathcal{D}}_h)\mathcal{E}_h^{0}\rangle_{p\times\widetilde{p}}.
\end{aligned}$$

Lemma 4.9 and the CFL condition (4.19) then provide the bounds for this term. Similarly, we use for $\gamma>0$ sufficently small that

$$\frac{\tau^2}{4}|\langle\boldsymbol{\mathcal{S}}_h^{1/2}\partial_\tau\widetilde{D}^{\ell+1},\boldsymbol{\mathcal{S}}_h^{1/2}\overline{\mathcal{E}}_h^{\ell+1}\rangle_{p\times\widetilde{p}}|\le C_\gamma\tau^4\|\boldsymbol{\mathcal{S}}_h^{1/2}\partial_\tau\widetilde{D}^{n+1}\|_{X_h^*}^2+\gamma|e_h^{\ell+1}+e_h^{\ell}|_{s_h^p}^2,$$

and thus the stabilization part can be absorbed into the left-hand side. Finally, the mixed defect term is estimated combining Lemma 4.8 and 4.9, and the discrete Gronwall estimate [Emm99, Proposition 4.1] gives the desired bound. □

Remark 4.11. In principle one can also circumvent the summation-by-parts technique if the application of $\boldsymbol{\mathcal{A}}_h$ to the defect is bounded. But as soon as L^2-adjoints of traces come into play, this is not possible anymore.

5. Application to examples and numerical experiments

In this section, we finally apply the result obtained in Sections 3 and 4 to the examples presented before. Without explicitly stating this everywhere, the discrete derivatives can be bounded by the maximums norm of their continuous counterpart without any additional constants, see for example [DN24, Lemma 4.2].

5.1. **Thermoelastic string.** For the example in Section 2.1, we employ continuous finite elements of order k to both the heat and the wave part, and thus no stabilization is used. In addition, we use a conforming method and thus use the continuous bilinear forms also in the discrete case. In particular, Assumptions 3.2 and 3.3 are satisfied. Concerning the projections, we employ Ritz projection R_h and the L^2-projection π_h via $P_h=(\mathrm{R}_h,\pi_h)$ and $\widetilde{P}_h=\pi_h$. For the reference operators, we choose $J_h=(\mathrm{R}_h,\mathrm{R}_h)$ and $\widetilde{J}_h=\mathrm{R}_h$. All the upcoming approximation results can be found in the book [BS08]. For the initial values and the right-hand side, we employ the interpolation $\mathcal{I}_h$. To shorten notation for linear elements, we set $k^*=\max\{k,2\}$, and can thus conclude for the initial data and the sources

$$\begin{aligned}
\|e_h(0)\|_{X_h}+\|\epsilon_h(0)\|_{X_h}&\lesssim h^k\big(|\partial_t u|_{H^k}+|\partial_t^2 u|_{H^{k^*}}+|\partial_t\theta|_{H^{k^*}}\big),\\
\|\Delta f\|_{X_h^*}+\|\Delta g\|_{H_h^*}&\lesssim h^{k+1}\big(|f|_{H^{k+1}}+|g|_{H^{k+1}}\big).
\end{aligned}$$

Further, by the choice of the reference operators, we further obtain

$$\|\Delta p(\partial_t x)\|_{X_h^*}+\|\Delta\widetilde{p}(\partial_t\theta)\|_{H_h^*}\lesssim h^{k+1}\big(|\partial_t^2 u|_{H^{k+1}}+|\partial_t\theta|_{H^{k+1}}\big).$$

For this problem, we use the fact that $X_h \subset Y$ holds, and thus obtain

$$\begin{aligned}|\Delta_{s,b}(x,\theta,e_h)| &= |s_h(J_h x, e_h) + \widetilde{b}_h(\widetilde{J}_h\theta, e_h) - s(x,e_h) - \widetilde{b}(\theta,e_h)| \\ &\le |s(J_h x - x, e_h)| + |\widehat{b}(\widetilde{J}_h\theta - \theta, e_h)| \\ &\lesssim h^k |\theta|_{H^{k+1}} \|e_h\|_{X_h},\end{aligned}$$

where we used the definition of J_h in the last step. Similarly, we compute using the definition of $\widetilde{J}_h$

$$\|\widetilde{\Delta}_{s,b}(x,\theta)\|_{H_h^*} \le \|\widetilde{s}(\widetilde{J}_h\theta - \theta, \cdot)\|_{H_h^*} + \|\widetilde{b}(\cdot, J_h x - x)\|_{H_h^*} \lesssim h^k |\partial_t u|_{H^{k+1}}.$$

Collecting all this, we obtain for a sufficiently smooth solution the spatial discretization error bound of optimal order as

$$\|u(t) - u_h(t)\|_{H_0^1} + \|\partial_t u(t) - \partial_t u_h(t)\|_{L^2} + \|\theta(t) - \theta_h(t)\|_{L^2} \lesssim h^k$$

with constants independent of h, and the full discretization error bound

$$\|u(t_n) - u^n\|_{H_0^1} + \|\partial_t u(t_n) - v_h^n\|_{L^2} + \|\theta(t_n) - \theta_h^n\|_{L^2} \lesssim \tau^2 + h^r$$

with constants independent of h and τ, where the last estimate holds under the CFL condition (4.19).

5.2. **Non-local in time visco-elasticity and acoustics.** For the example in Section 2.2, we only discuss the visco-elastic case, since the acoustic equation can be treated by minor modifications of the considerations below. We apply discontinuous elements for the velocity part and continuous elements for the pressure part. Further, the coupling term is discretized in a conforming way, by leaving the derivative on the continuous elements. For the bilinear forms p_h, $\widetilde{p}_h$, and $\widetilde{s}_h$ we simply use the restriction of the continuous forms to the (broken) polynomial spaces. In particular, we chose broken polynomial spaces of order k and div-conforming elements of order $\ell \le k+1$, for example Raviart–Thomas elements, such that the image under the divergence is contained in the broken polynomial space of degree $\ell - 1$. For the bilinear form s_h, we follow the discretization of Section 4 in [HPS+15], using the discrete operator A_h there to define $s_h(x_h, y_h) = (A_h x_h, y_h)$, which we then decompose as $s_h = s_h^s + s_h^p$, see the definitions in (A.5) and (A.6) in Appendix A. Further, Lemma A.1 implies that Assumption 3.2 is satisfied. We choose for the wave part all projections to be the component-wise broken L^2-projections, which gives $e_h(0) = \Delta p(\partial_t x) = \Delta\widetilde{p}(\partial_t\theta) = \Delta f = 0$. The projection $\widetilde{J}_h$ for the heat part is chosen as the div-conforming interpolation which satisfies a commuting diagram property with the broken polynomial spaces. The initial values and the right-hand side are computed by this interpolation, and thus it holds

$$\|\epsilon_h(0)\|_{X_h} + \|\Delta g\|_{H_h^*} \lesssim h^\ell \big(\|\theta\|_{H^\ell} + \|g\|_{H^\ell}\big).$$

Further, we have

$$\begin{aligned}|\widetilde{\Delta}_{s,b}(x,\theta,\varphi_h)| &\le |\widetilde{s}(\widetilde{J}_h\theta - \theta, \varphi_h)| + |\widetilde{b}(\varphi_h, x - J_h x)| \\ &\lesssim \|\widetilde{J}_h\theta - \theta\|_{L^2} \|\varphi_h\|_{L^2} \\ &\lesssim h^\ell \|\theta\|_{H^\ell} \|\varphi_h\|_{L^2},\end{aligned}$$

where we used the best-approximation property, see e.g., [Mon03, Theorem 5.25]. In addition, we obtain

$$\widetilde{b}(\varphi_h, x - J_h x) = \sum_{i=1}^{G} \langle \operatorname{div} \boldsymbol{\sigma}_{h,i}, J_h x - x \rangle_{L^2} = 0,$$

since $\operatorname{div} \boldsymbol{\sigma}_{h,i}$ is an element of the broken polynomial space of degree $\ell - 1 \leq k$, and hence orthogonal on the projection error. For the differential parts, we use Assumption 3.3 and obtain

$$\begin{aligned} |\Delta_{s,b}(x, \theta, e_h)| &= |s_h(J_h x, e_h) + \widetilde{b}_h(\widetilde{J}_h \theta, e_h) - \widehat{s}(x, e_h) - \widehat{b}(\theta, e_h)| \\ &\leq |s_h(J_h x - x, e_h)| + |\widetilde{b}_h(\widetilde{J}_h \theta - \theta, e_h)|. \end{aligned}$$

In Appendix A Lemma A.2, we provide the estimate

$$|s_h(J_h x - x, e_h)| \leq C h^{k+1/2} |x|_{H^{k+1}} |e_h|_{s_h^p}. \tag{5.1}$$

Finally, we have by the commuting diagram property

$$\begin{aligned} |\widetilde{b}_h(\widetilde{J}_h \theta - \theta, e_h)| &= |\sum_{i=1}^{G} \langle \operatorname{div}(\widetilde{J}_h - I) \boldsymbol{\sigma}_i, e_h \rangle_{L^2}| \\ &= |\sum_{i=1}^{G} \langle (\pi_h - I) \operatorname{div} \boldsymbol{\sigma}_i, e_h \rangle_{L^2}| \\ &\lesssim h^{\ell} |e_h|_{X_h} \sum_{i=1}^{G} |\operatorname{div} \boldsymbol{\sigma}_i|_{H^{k+1}}. \end{aligned}$$

In total, we can thus conclude that for a sufficiently smooth solution the spatial discretization error bound of optimal order as

$$\|\boldsymbol{v}(t) - \boldsymbol{v}_h(t)\|_{L^2} + \|\boldsymbol{\sigma}_0(t) - \boldsymbol{\sigma}_{0,h}(t)\|_{L^2} + \sum_{i=1}^{G} \|\boldsymbol{\sigma}_i(t) - \boldsymbol{\sigma}_{i,h}(t)\|_{L^2} \lesssim h^{\ell} + h^{k+1/2},$$

with constants independent of h, and the full discretization error bound

$$\|\boldsymbol{v}(t_n) - \boldsymbol{v}_h^n\|_{L^2} + \|\boldsymbol{\sigma}_0(t_n) - \boldsymbol{\sigma}_{0,h}^n\|_{L^2} + \sum_{i=1}^{G} \|\boldsymbol{\sigma}_i(t_n) - \boldsymbol{\sigma}_{i,h}^n\|_{L^2} \lesssim \tau^2 + h^{\ell} + h^{k+1/2},$$

with constants independent of h and τ, where the last estimate holds under the CFL condition (4.19). The typical choices for ℓ are k or $k+1$.

5.3. **Thermo-elastic wave coupling.** For the third example in Section 2.3, we choose the same discretization as in Section 5.2 for the wave part, and again obtain with the component-wise broken L^2-projections that $e_h(0) = \Delta p(\partial_t x) = \Delta \widetilde{p}(\partial_t \theta) = \Delta f = 0$. For the heat part we employ (continuous) Lagrange finite elements of order $\ell \leq k+1$ and choose for $\widetilde{J}_h$ the Ritz projection, and for the initial values and the right-hand side the nodal interpolation, which directly yields

$$\|\epsilon_h(0)\|_{X_h} + \|\Delta g\|_{H_h^*} \lesssim h^{\ell+1} \big(\|\theta\|_{H^{\ell+1}} + \|g\|_{H^{\ell+1}} \big).$$

Further, we have

$$|\widetilde{\Delta}_{s,b}(x, \theta, \varphi_h)| \leq |\widetilde{s}(\widetilde{J}_h \theta - \theta, \varphi_h)| + |\widetilde{b}(\varphi_h, x - J_h x)| = 0,$$

using the definition of the Ritz projection and again the fact that $\nabla\varphi_h$ is in the space of broken polynomials or oder $\ell - 1 \leq k$, such that the orthogonalality

$$\widetilde{b}(\varphi_h, x - J_h x) = \alpha\langle\nabla\varphi_h, x - J_h x\rangle_{L^2} = 0$$

holds. Using the estimate in (5.1) for the upwind part, it remains to bound

$$|\widetilde{b}_h(\widetilde{J}_h\theta - \theta, e_h)| = |\langle\alpha\nabla(\widetilde{J}_h\theta - \theta), e_h\rangle_{L^2}| \lesssim h^\ell \|\theta\|_{H^{\ell+1}} \|e_h\|_{X_h}.$$

As for the previous example, we thus obtain for a sufficiently smooth solution the spatial discretization error bound of optimal order as

$$\|\boldsymbol{v}(t) - \boldsymbol{v}_h(t)\|_{L^2} + \|\boldsymbol{\sigma}(t) - \boldsymbol{\sigma}_h(t)\|_{L^2} + \|\theta(t) - \theta_h(t)\|_{L^2} \lesssim h^\ell + h^{k+1/2}$$

with constants independent of h, and the full discretization error bound

$$\|\boldsymbol{v}(t_n) - \boldsymbol{v}_h^n\|_{L^2} + \|\boldsymbol{\sigma}(t_n) - \boldsymbol{\sigma}_h^n\|_{L^2} + \|\theta(t_n) - \theta_h^n\|_{L^2} \lesssim \tau^2 + h^\ell + h^{k+1/2},$$

with constants independent of h and τ, where the last estimate holds under the CFL condition (4.19). The typical choices for ℓ are k or $k+1$.

5.4. **Maxwell equation with dissipative 2D material.** Finally, for the example in Section 2.4 we apply a dG method with central flux (upwind could be included as well) to the Maxwell part x and use its restriction to the interface as the ansatz space for θ. To be precise, we use the space of broken polynomials of degree k for X_h, which yields again a broken polynomial space of degree k on the (lower dimensional) restriction to the interface. This leads to the standard dG Maxwell operators in s_h, which can for example be found in [HS19, Section 4.2], and thus Assumption 3.2 is satisfied. For the coupling form b_h, we set

$$\widetilde{b}_h(\varphi_h, y_h) = \widetilde{p}(\varphi_h, \{\!\{\mathbb{1}_\ell \otimes y_{h,1,\parallel}\}\!\}),$$

for $y_h \in X_h$ and $\varphi_h \in H_h$. We note that the exact solution satisfies the generalized consistency condition of Assumption 3.3, see [DDH26, Lem. 3.10 (2)] for an analogous statement of external surface currents.

We now study the error terms in (3.4) appearing in Theorem 3.4, and choose the standard L^2-projections in all cases. This immediately implies that $e_h(0) = \epsilon_h(0) = 0$, and similarly, as we work in the correct inner products also $\Delta p(\partial_t x) = \Delta\widetilde{p}(\partial_t\theta) = 0$. In the same manner, if we compute the sources f_h and g_h via projections, we also have $\Delta f = \Delta g = 0$. As in the elastic cases, Assumption 3.3 yields

$$\begin{aligned}|\Delta_{s,b}(x, \theta, e_h)| &= |s_h(J_h x, e_h) + \widetilde{b}_h(\widetilde{J}_h\theta, e_h) - \widehat{s}(x, e_h) - \widehat{b}(\theta, e_h)| \\ &= |s_h(J_h x - x, e_h) + \widetilde{b}_h(\widetilde{J}_h\theta - \theta, e_h)|.\end{aligned}$$

The remaining term, can be estimated using [HS16, eq. (5.5)], as

$$|\Delta_{s,b}(x, \theta, e_h)| \lesssim h^k\big(|x|_{H^{k+1}} + |\theta|_{H^{k+1}}\big)\|e_h\|_{X_h}.$$

Finally, we assume that solution if sufficiently regular, and note the best approximation results in [EG21, Section 18.4]. Then, we obtain for the spatial discretization the estimate

$$\|E(t) - E_h(t)\|_{L^2} + \|H(t) - H_h(t)\|_{L^2} + \|\theta(t) - \theta_h(t)\|_{L^2} \lesssim h^k$$

with constants independent of h, and for the fully discrete scheme

$$\|E(t_n) - E_h^n\|_{L^2} + \|H(t_n) - H_h^n\|_{L^2} + \|\theta(t_n) - \theta_h^n\|_{L^2} \lesssim \tau^2 + h^k,$$

with constants independent of h and τ, where the last estimate holds under the CFL condition (4.19).

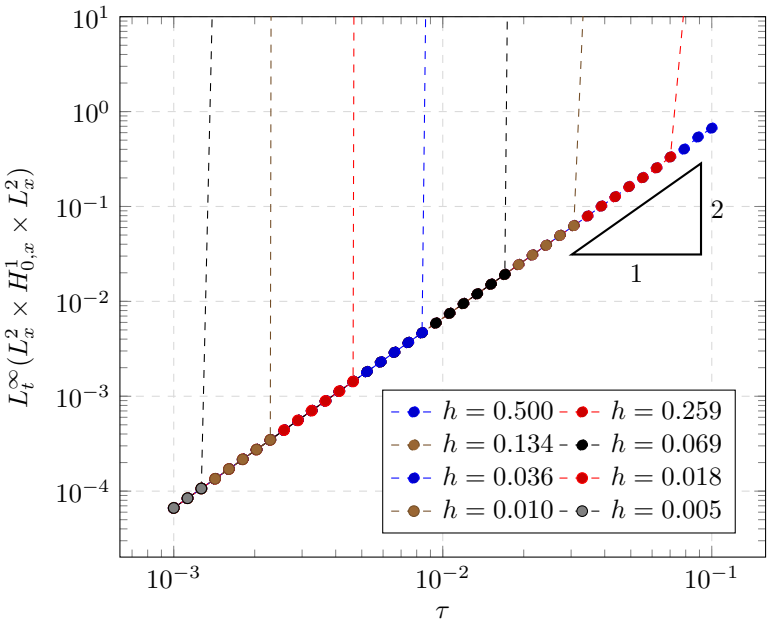

FIGURE 1. L^∞-error in time and the $L^2 \times H_0^1 \times L^2$ error in space of the exact solution (6.1) against the time-step size τ.

6. Numerical experiments

In this section, we present some numerical experiments for the thermoelastic string from Section 2.1. We show convergence in space and time as well as study the behavior of the CFL condition stated in Assumption 4.4. The codes to reproduce the experiments are available on request.

6.1. **Thermoelastic string.** We consider the example from Section 2.1. We first verify second-order convergence in time and Assumption 4.4. Therefore, let

$$x_2(t,x) = e^t \cos(\omega t) x(1-x), \qquad \theta(t,x) = e^t \sin(\eta t) x(1-x), \tag{6.1}$$

and choose f and g such that the $\mathcal{U} = (x_1, x_2, \theta)$ solves (2.4). In the following examples we set $\omega = 3.37 \cdot \pi$, $\eta = 2.3 \cdot \pi$ and the final time $T = 1.0$. Note that the exact solution is a second-order polynomial in space and is therefore represented exactly by second-order ansatz functions on any mesh. Consequently, we only measure the temporal integration error in the experiments below. For a series of eight mesh sizes ranging from 0.5 to 0.005, we compute the L^∞-error in time and the $L^2 \times H_0^1 \times L^2$ error in space against the exact solution, using 40 different time-step sizes between 0.1 and 0.001. The results are displayed in Figure 1. We conclude that our method exhibits second-order convergence in time.

In the next example, we determine the threshold time step τ_{CFL} for which our method is *stable*. For a given target mesh size h_{target} we choose a sufficiently large interval $\tau_{\mathrm{CFL}} \in [\tau_{\mathrm{low}}, \tau_{\mathrm{high}}]$ such that the method is *unstable* at τ_{high} and *stable* at τ_{low} when compared with a reference calculation using a mesh size $h_{\mathrm{ref}} = 1.0$. Using the bisection method we halve the interval and repeat the comparison at each step

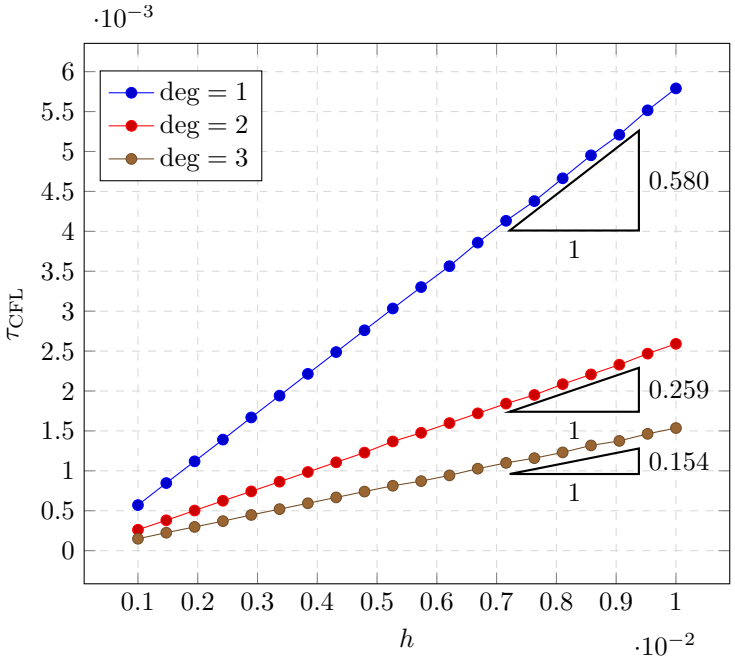

FIGURE 2. Approximation of τ_{CFL} plotted against the mesh size h.

until the interval width falls below 10^{-5}. The midpoint of the final interval is then taken as an approximation of τ_{CFL}. Figure 2 shows the results of this procedure for 20 different target mesh sizes ranging from 0.1 to 0.001 and different polynomial degrees of ansatz functions. From these data we conclude that the method is stable for all time-step sizes $\tau < \tau_{\mathrm{CFL}} \approx h$.

The next example verifies the convergence order in space. We define a different exact solution, i.e.

$$x_2(t,x) = t\sin(3\pi x)e^{-20(x-\frac{1}{2})^2}, \qquad \theta(t,x) = t\sin(4\pi x)e^{-20(x-\frac{1}{2})^2}, \tag{6.2}$$

and choose again x_1, f and g such that the collection is a solution of (2.4). Note that the exact solution is polynomial in time and therefore integrated exactly by our scheme. Hence, we only measure the space discretization error in the experiment below. For a sequence of 40 different mesh sizes, we calculate the error against the exact solution with a time step size of 0.001. Figure 3 shows the result of this experiment and confirms our findings from above.

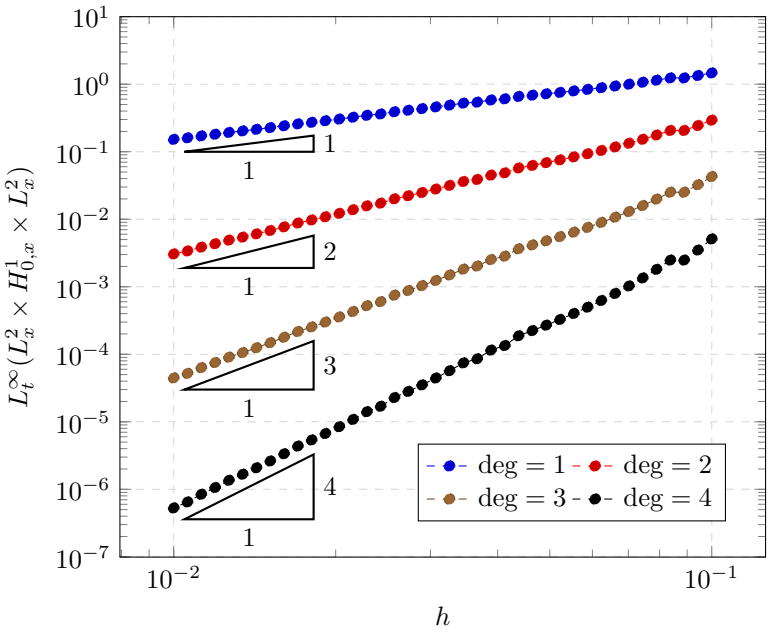

FIGURE 3. L^∞-error in time and the $L^2 \times H_0^1 \times L^2$ error in space of the exact solution (6.2) against the mesh size h for $\tau = 0.001$.

REFERENCES

[ACL18] F. Assous, P. Ciarlet, and S. Labrunie. *Mathematical foundations of computational electromagnetism*, volume 198 of *Applied Mathematical Sciences*. Springer, Cham, 2018.

[BGN14] T. Bodnar, G. P. Galdi, and S. Necasova, editors. *Fluid-Structure Interaction and Biomedical Applications*. Advances in Mathematical Fluid Mechanics. Springer, Basel, Switzerland, 2014 edition, October 2014.

[BS08] S. C. Brenner and L. R. Scott. *The mathematical theory of finite element methods*, volume 15 of *Texts in Applied Mathematics*. Springer, New York, third edition, 2008.

[DDH26] B. Dörich, J. Dörner, and M. Hochbruck. Error analysis of DGTD for linear Maxwell equations with inhomogeneous interface conditions. *Math. Comp.*, pages 1–31, 2026. Online first.

[DFW16] W. Dörfler, S. Findeisen, and C. Wieners. Space-time discontinuous Galerkin discretizations for linear first-order hyperbolic evolution systems. *Comput. Methods Appl. Math.*, 16(3):409–428, 2016.

[DK06] M. Dumbser and M. Käser. An arbitrary high-order discontinuous galerkin method for elastic waves on unstructured meshes — ii. the three-dimensional isotropic case. *Geophysical Journal International*, 167(1):319–336, 10 2006.

[DN24] B. Dörich and V. Nikolić. Robust fully discrete error bounds for the Kuznetsov equations in the inviscid limit. CRC 1173 Preprint 2024/1, Karlsruhe Institute of Technology, jan 2024. Revised version of October 2025.

[DWZ19] W. Dörfler, C. Wieners, and D. Ziegler. Parallel adaptive discontinuous galerkin discretizations in space and time for linear elastic and acoustic waves. In Ulrich Langer and Olaf Steinbach, editors, *Space-Time Methods: Applications to Partial Differential Equations*, volume 25 of *Radon Series on Computational and Applied Mathematics*, pages 61–88, Berlin/Boston, 2019. De Gruyter.

[EG21] A. Ern and J.-L. Guermond. *Finite elements I—Approximation and interpolation*, volume 72 of *Texts in Applied Mathematics*. Springer, Cham, [2021] ©2021.

[Emm99] E. Emmrich. Discrete versions of Gronwall's lemma and their application to the numerical analysis of parabolic problems. Preprint no. 637, Fachbereich Mathematik, TU Berlin, 1999.

[FLLP05] L. Fezoui, S. Lanteri, S. Lohrengel, and S. Piperno. Convergence and stability of a discontinuous Galerkin time-domain method for the 3D heterogeneous Maxwell equations on unstructured meshes. *M2AN Math. Model. Numer. Anal.*, 39(6):1149–1176, 2005.

[HHS19] D. Hipp, M. Hochbruck, and C. Stohrer. Unified error analysis for nonconforming space discretizations of wave-type equations. *IMA J. Numer. Anal.*, 39(3):1206–1245, 2019.

[HPS+15] M. Hochbruck, T. Pažur, A. Schulz, E. Thawinan, and C. Wieners. Efficient time integration for discontinuous Galerkin approximations of linear wave equations [Plenary lecture presented at the 83rd Annual GAMM Conference, Darmstadt, 26th–30th March, 2012]. *ZAMM Z. Angew. Math. Mech.*, 95(3):237–259, 2015.

[HS16] M. Hochbruck and A. Sturm. Error analysis of a second-order locally implicit method for linear Maxwell's equations. *SIAM J. Numer. Anal.*, 54(5):3167–3191, 2016.

[HS19] M. Hochbruck and A. Sturm. Upwind discontinuous Galerkin space discretization and locally implicit time integration for linear Maxwell's equations. *Math. Comp.*, 88(317):1121–1153, 2019.

[HSVSW19] G. C. Hsiao, T. Sánchez-Vizuet, F.-J. Sayas, and R. J. Weinacht. A time-dependent wave-thermoelastic solid interaction. *IMA J. Numer. Anal.*, 39(2):924–956, 2019.

[HW02] J. S. Hesthaven and T. Warburton. Nodal high-order methods on unstructured grids. I. Time-domain solution of Maxwell's equations. *J. Comput. Phys.*, 181(1):186–221, 2002.

[IOS10] J. Ignaczak and M. Ostoja-Starzewski. *Thermoelasticity with finite wave speeds*. Oxford Mathematical Monographs. Oxford University Press, Oxford, 2010.

[JR00] S. Jiang and R. Racke. *Evolution equations in thermoelasticity*, volume 112 of *Chapman & Hall/CRC Monographs and Surveys in Pure and Applied Mathematics*. Chapman & Hall/CRC, Boca Raton, FL, 2000.

[KD06] M. Käser and M. Dumbser. An arbitrary high-order discontinuous galerkin method for elastic waves on unstructured meshes — i. the two-dimensional isotropic case with external source terms. *Geophysical Journal International*, 166(2):855–877, 08 2006.

[KGBB79] V. D. Kupradze, T. G. Gegelia, M. O. Basheleishvili, and T. V. Burchuladze. *Three-dimensional problems of the mathematical theory of elasticity and thermoelasticity*, volume 25 of *North-Holland Series in Applied Mathematics and Mechanics*. North-Holland Publishing Co., Amsterdam-New York, russian edition, 1979. Edited by V. D. Kupradze.

[LS13] S. Lanteri and C. Scheid. Convergence of a discontinuous Galerkin scheme for the mixed time-domain Maxwell's equations in dispersive media. *IMA J. Numer. Anal.*, 33(2):432–459, 2013.

[LT12] W. Layton and C. Trenchea. Stability of two IMEX methods, CNLF and BDF2-AB2, for uncoupling systems of evolution equations. *Appl. Numer. Math.*, 62(2):112–120, 2012.

[Mon03] P. Monk. *Finite element methods for Maxwell's equations*. Numerical Mathematics and Scientific Computation. Oxford University Press, New York, 2003.

[Zie20] D. A. Ziegler. *A parallel and adaptive space-time discontinuous Galerkin method for visco-elastic and visco-acoustic waves*. PhD thesis, Karlsruher Institut für Technologie (KIT), 2020.

Appendix A. Computations for the examples

A.1. **Elastic example.** In Section 5.2 and 5.3 we suggest a discontinuous Galerkin discretization of the forms

$$\begin{aligned} p &: X \times X \to \mathbb{R}, & p(x,y) &= \langle \rho \boldsymbol{v}, \boldsymbol{w} \rangle_{L^2} + \langle C^{-1} \boldsymbol{\sigma}, \boldsymbol{\lambda} \rangle_{L^2}, \\ s &: Y \times Y \to \mathbb{R}, & s(x,y) &= -\langle \operatorname{div} \boldsymbol{\sigma}, \boldsymbol{w} \rangle_{L^2} - \langle \epsilon(\boldsymbol{v}), \boldsymbol{\lambda} \rangle_{L^2}, \end{aligned}$$

where $x = (\boldsymbol{v}, \boldsymbol{\sigma})$ and $y = (\boldsymbol{w}, \boldsymbol{\lambda})$ with $x, y \in Y = H_0^1(\Omega, \mathbb{R}^d) \times H(\mathrm{div}, \Omega, \mathbb{R}^{d\times d}_{\mathrm{sym}})$ and $\epsilon(\boldsymbol{v}) = \mathrm{Sym}(D\boldsymbol{v})$ denotes the symmetric gradient. Our presentation follows [Zie20, HPS$^+$15]. Starting from their local discretization, we derive global dG forms and prove the necessary auxiliary result for the analysis of our examples.

We restrict us in the following to dimension $d = 2$ and assume that the elasticity tensor describes an isotropic media, i.e.

$$Cw = C(\mu, \lambda)w = 2\mu w + \lambda \,\mathrm{tr}(w) I,$$

with Lamé parameters $\lambda \geq 0$, $\mu > 0$.

Let $\mathcal{T}_h$ be a matching triangulation of Ω and denote with Y_h the space of broken polynomials of degree $k > 0$ on this mesh. All problem dependent constants are assumed to be constant on every $K \in \mathcal{T}_h$. In the following, we introduce a local and a global naming convention of mesh faces and trace-quantities of functions on them.

For any element $K \in \mathcal{T}_h$, we define the set of faces F associated to K as $\mathcal{F}_K$. For any face $F \in \mathcal{F}_K$, there is an associated outer unit normal vector $n_{K,F}$ and a unit tangential vector, chosen with respect to the right-hand rule, and denoted with $\tau_{K,F}$. The element opposite of K on the face F, if existent, is denoted with K_F. Local jumps and averages are defined as

$$[\![f]\!]_{K,F} = (f\big|_{K_F})\big|_F - (f\big|_K)\big|_F, \qquad \{\{f\}\}^\alpha_{K,F} = \alpha^{K_F}(f\big|_{K_F})\big|_F + \alpha^K (f\big|_K)\big|_F,$$

where $\alpha^{K_F}, \alpha^K > 0$ denote positive weights such that $\alpha_{K,F} + \alpha_K = 1$. The definition is understood element-wise for vector- and tensor-valued functions.

The set of all mesh faces is denoted as $\mathcal{F}_h$. The latter set is further divided in the set $\mathcal{F}_h^{\mathrm{int}}$ of interior faces and $\mathcal{F}_h^{\mathrm{bnd}}$ of boundary faces. For any face $F \in \mathcal{F}_h^{\mathrm{int}}$, we fix a global numbering scheme, i.e., we choose and ordered tuple $(K_1, K_2) \in \mathcal{T}_h \times \mathcal{T}_h$ such that $F \in \mathcal{F}_{K_1} \cap \mathcal{F}_{K_2}$. Based on this numbering, we define the global unit normal and tangential vectors as

$$n_F = n_{K_1,F} = -n_{K_2,F}, \qquad \tau_F = \tau_{K_1,F} = -\tau_{K_2,F}. \tag{A.1}$$

Similar, we define global jump and average as

$$[\![f]\!]_F = [\![f]\!]_{K_1,F} = -[\![f]\!]_{K_2,F}, \qquad \{\{f\}\}^\alpha_F = \{\{f\}\}^\alpha_{K_1,F} = \{\{f\}\}^\alpha_{K_2,F}. \tag{A.2}$$

Compare Figure 4 for our naming convention.

Following the work in [HPS$^+$15, Zie20], we obtain the local definition of the operator $S_h = S_h^s + S_h^p$ on every $K \in \mathcal{T}_h$, for $x_h = (\boldsymbol{v}_h, \boldsymbol{\sigma}_h)$ and $y_h = (\boldsymbol{w}_h, \boldsymbol{\lambda}_h)$ with $x_h, y_h \in Y_h$

$$\begin{aligned}
&\langle S_h^s x_h, y_h\rangle_{L^2(K)} \\
&\quad = -\langle \mathrm{div}\,\boldsymbol{\sigma}_h, \boldsymbol{w}_h\rangle_{L^2(K)} - \langle \epsilon(\boldsymbol{v}_h), \boldsymbol{\lambda}_h\rangle_{L^2(K)} \\
&\qquad - \sum_{F\in\mathcal{F}_K} \alpha_2^{K,F} \langle n_{K,F}\cdot([\![\boldsymbol{\sigma}_h]\!]_{K,F} n_{K,F}), n_{K,F}\cdot \boldsymbol{w}_h\rangle_{L^2(F)} \\
&\qquad\qquad + \alpha_3^{K,F} \langle n_{K,F}\cdot [\![\boldsymbol{v}_h]\!]_{K,F}, n_{K,F}\cdot(\boldsymbol{\lambda}_h n_{K,F})\rangle_{L^2(F)} \\
&\qquad - \sum_{F\in\mathcal{F}_K} \alpha_6^{K,F} \langle \tau_{K,F}\cdot([\![\boldsymbol{\sigma}_h]\!]_{K,F} n_{K,F}), \tau_{K,F}\cdot \boldsymbol{w}_h\rangle_{L^2(F)} \\
&\qquad\qquad + \alpha_7^{K,F} \langle \tau_{K,F}\cdot [\![\boldsymbol{v}_h]\!]_{K,F}, \tau_{K,F}\cdot(\boldsymbol{\lambda}_h n_{K,F})\rangle_{L^2(F)},
\end{aligned} \tag{A.3}$$

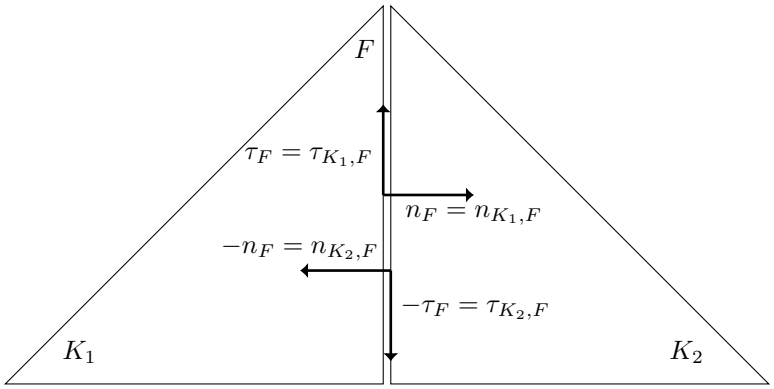

FIGURE 4. Face naming convention with normal and tangential vectors.

$$
\begin{aligned}
&\langle S_h^p x_h, y_h \rangle_{L^2(K)} \\
&\quad = -\sum_{F \in \mathcal{F}_K} \alpha_1^F \langle n_{K,F} \cdot (\llbracket \boldsymbol{\sigma}_h \rrbracket_{K,F} n_{K,F}), n_{K,F} \cdot (\boldsymbol{\lambda}_h n_{K,F}) \rangle_{L^2(F)} \\
&\qquad + \alpha_4^F \langle n_{K,F} \cdot \llbracket \boldsymbol{v}_h \rrbracket_{K,F}, n_{K,F} \cdot \boldsymbol{w}_h \rangle_{L^2(F)} \\
&\quad - \sum_{F \in \mathcal{F}_K} \alpha_5^F \langle \tau_{K,F} \cdot (\llbracket \boldsymbol{\sigma}_h \rrbracket_{K,F} n_{K,F}), \tau_{K,F} \cdot (\boldsymbol{\lambda}_h n_{K,F}) \rangle_{L^2(F)} \\
&\qquad + \alpha_8^F \langle \tau_{K,F} \cdot \llbracket \boldsymbol{v}_h \rrbracket_{K,F}, \tau_{K,F} \cdot \boldsymbol{w}_h \rangle_{L^2(F)},
\end{aligned}
\tag{A.4}
$$

with constants

$$
\begin{aligned}
\alpha_1^F &= \frac{1}{\rho_K c_{P,K} + \rho_{K_F} c_{P,K_F}}, & \alpha_2^{K,F} &= \frac{\rho_K c_{P,K}}{\rho_K c_{P,K} + \rho_{K_F} c_{P,K_F}}, \\
\alpha_3^{K,F} &= \frac{\rho_{K_F} c_{P,K_F}}{\rho_K c_{P,K} + \rho_{K_F} c_{P,K_F}}, & \alpha_4^F &= \frac{\rho_K c_{P,K} \rho_{K_F} c_{P,K_F}}{\rho_K c_{P,K} + \rho_{K_F} c_{P,K_F}}, \\
\alpha_5^F &= \frac{1}{\rho_K c_{S,K} + \rho_{K_F} c_{S,K_F}}, & \alpha_6^{K,F} &= \frac{\rho_K c_{S,K}}{\rho_K c_{S,K} + \rho_{K_F} c_{S,K_F}}, \\
\alpha_7^{K,F} &= \frac{\rho_{K_F} c_{S,K_F}}{\rho_K c_{S,K} + \rho_{K_F} c_{S,K_F}}, & \alpha_8^F &= \frac{\rho_K c_{S,K} \rho_{K_F} c_{S,K_F}}{\rho_K c_{S,K} + \rho_{K_F} c_{S,K_F}},
\end{aligned}
$$

where c_P and c_S denotes the velocity of shear and pressure waves, defined as

$$
c_P = \sqrt{\frac{2\mu/3 + \lambda}{\rho}}, \qquad c_S = \sqrt{\frac{\mu}{\rho}}.
$$

On a boundary face $F \in \mathcal{F}_h^{\text{bnd}}$ we define $\llbracket \boldsymbol{v}_h \rrbracket_{K,F} = -2x_{h,1}\big|_F$, $\llbracket \boldsymbol{\sigma}_h \rrbracket_{K,F} = 0$, $\rho_{K_F} = \rho_K$, $c_{S,K_F} = c_{S,K}$ and $c_{P,K_F} = c_{P,K}$.

Summing in (A.3) and (A.4) over all elements $K \in \mathcal{T}_h$ while using (A.1), (A.2) yields the global operators

$$
\begin{aligned}
&\langle S_h^s x_h, y_h\rangle_{L^2(\Omega)} \\
&\quad = -\sum_{K\in\mathcal{T}_h} \langle \operatorname{div}\boldsymbol{\sigma}_h, \boldsymbol{w}_h\rangle_{L^2(K)} + \langle \epsilon(\boldsymbol{v}_h), \boldsymbol{\lambda}_h\rangle_{L^2(K)} \\
&\qquad - \sum_{F\in\mathcal{F}_h^{\mathrm{int}}} \langle n_F\cdot([\![\boldsymbol{\sigma}_h]\!]_F n_F), n_F\cdot\{\{\boldsymbol{w}_h\}\}_F^{\alpha_2}\rangle_{L^2(F)} \\
&\qquad\qquad + \langle n_F\cdot[\![\boldsymbol{v}_h]\!]_F, n_F\cdot(\{\{\boldsymbol{\lambda}_h\}\}_F^{\alpha_3} n_F)\rangle_{L^2(F)} \\
&\qquad\qquad + \langle \tau_F\cdot([\![\boldsymbol{\sigma}_h]\!]_F n_F), \tau_F\cdot\{\{\boldsymbol{w}_h\}\}_F^{\alpha_6}\rangle_{L^2(F)} \\
&\qquad\qquad + \langle \tau_F\cdot[\![\boldsymbol{v}_h]\!]_F, \tau_F\cdot(\{\{\boldsymbol{\lambda}_h\}\}_F^{\alpha_7} n_F)\rangle_{L^2(F)}, \\
&\qquad + \sum_{F\in\mathcal{F}_h^{\mathrm{bnd}}} \langle n_F\cdot\boldsymbol{v}_h, n_F\cdot(\boldsymbol{\lambda}_h n_F)\rangle_{L^2(F)} \\
&\qquad\qquad + \langle \tau_F\cdot\boldsymbol{v}_h, \tau_F\cdot(\boldsymbol{\lambda}_h n_F)\rangle_{L^2(F)},
\end{aligned}
\tag{A.5}
$$

$$
\begin{aligned}
&\langle S_h^p x_h, y_h\rangle_{L^2(\Omega)} \\
&\quad = \sum_{F\in\mathcal{F}_h^{\mathrm{int}}} \alpha_1^F \langle n_F\cdot([\![\boldsymbol{\sigma}_h]\!]_F n_F), n_F\cdot([\![\boldsymbol{\lambda}_h]\!]_F n_F)\rangle_{L^2(F)} \\
&\qquad\qquad + \alpha_4^F \langle n_F\cdot[\![\boldsymbol{v}_h]\!]_F, n_F\cdot[\![\boldsymbol{w}_h]\!]_F\rangle_{L^2(F)} \\
&\qquad\qquad + \alpha_5^F \langle \tau_F\cdot([\![\boldsymbol{\sigma}_h]\!]_F n_F), \tau_F\cdot([\![\boldsymbol{\lambda}_h]\!]_F n_F)\rangle_{L^2(F)} \\
&\qquad\qquad + \alpha_8^F \langle \tau_F\cdot[\![\boldsymbol{v}_h]\!]_F, \tau_F\cdot[\![\boldsymbol{w}_h]\!]_f\rangle_{L^2(F)}, \\
&\qquad + \sum_{F\in\mathcal{F}_h^{\mathrm{bnd}}} \rho_F c_{P,F}\langle n_F\cdot\boldsymbol{v}_h, n_F\cdot\boldsymbol{w}_h\rangle_{L^2(F)} \\
&\qquad\qquad + \quad \rho_F c_{S,F}\langle \tau_F\cdot\boldsymbol{v}_h, \tau_F\cdot\boldsymbol{w}_h\rangle_{L^2(F)}.
\end{aligned}
\tag{A.6}
$$

Lemma A.1. *The operators S_h^s and S_h^p, defined in* (A.5) *and* (A.6) *respectively, satisfy Assumption 3.2.*

Proof. Assumption 3.2 (a) is shown in [Zie20, Lem. 3.2]. Furthermore, from representation (A.6), we directly conclude that for any $y = (\boldsymbol{w}, \boldsymbol{\lambda}) \in Y$ it holds that

$$\langle S_h^p y, y_h\rangle_{L^2(\Omega)} = 0, \qquad \text{for all } y_h \in Y_h,$$

since $[\![\boldsymbol{w}]\!]_F = 0$ for $\boldsymbol{w} \in H_0^1(\Omega)$ and $[\![\boldsymbol{\lambda}]\!]_F n_F = 0$ for $\boldsymbol{\lambda} \in H(\operatorname{div}, \Omega, \mathbb{R}^{d\times d}_{\mathrm{sym}})$. Moreover, on any boundary face $F \in \mathcal{F}_h^{\mathrm{bnd}}$ it holds that $\boldsymbol{w}\big|_F = 0$. Hence, Assumption 3.2 (b) is satisfied. □

It remains to prove (5.1). Let $J_h : Y \to Y_h$ denote the broken L^2-orthogonal projection on $\mathcal{T}_h$, i.e., for $x \in Y$ it holds that

$$\langle J_h x - x, y_h\rangle_{L^2(K)} = 0, \quad \text{for all } K \in \mathcal{T}_h,\ y_h \in Y_h.$$

For any $x \in Y$ with $x\big|_K \in H^{k+1}(K)$, $K \in \mathcal{T}_h$, we have the approximation properties, see, e.g., [EG21, Sec. 18.4],

$$
\begin{aligned}
\|J_h x - x\|_{L^2(K)} &\le h_K^{k+1} |x|_{H^{k+1}(K)}, \\
\|J_h x - x\|_{L^2(F)} &\le h_K^{k+1/2} |x|_{H^{k+1}(K)}, \quad F \in \mathcal{F}_K.
\end{aligned}
\tag{A.7}
$$

Lemma A.2. *Let $x \in Y$ with $x\big|_K \in H^{k+1}(K)$, $K \in \mathcal{T}_h$. Then*

$$|s_h(J_h x - x, y_h)| \le h^{k+1/2}\Big(\sum_{K\in\mathcal{T}_h} |x|^2_{H^{k+1}(K)}\Big)^{1/2} |y_h|_{s_h^p}.$$

Proof. Let $x = (\boldsymbol{v}, \boldsymbol{\sigma})$ and $y_h = (\boldsymbol{w}_h, \boldsymbol{\lambda}_h)$. Since S_h^s is skew-adjoint it holds that $\langle S_h^s(J_h x - x), y_h\rangle_{L^2} = -\langle J_h x - x, S_h^s y_h\rangle_{L^2}$. Hence, for any $K \in \mathcal{T}_h$ the bulk terms in (A.5) vanish, i.e.

$$\langle \operatorname{div} \boldsymbol{\lambda}_h, J_{h,2}\boldsymbol{v} - \boldsymbol{v}\rangle_{L^2(K)} = \langle \epsilon(\boldsymbol{w}_h), J_{h,1}\boldsymbol{\sigma} - \boldsymbol{\sigma}\rangle_{L^2(K)} = 0,$$

by the definition of the broken L^2-projection. Thus, (A.5) only depends on faces, and we obtain with the Cauchy-Schwarz inequality that

$$\begin{aligned}
|\langle S_h^s(J_h x - x), y_h\rangle_{L^2}| &\\
&\lesssim \Big(\sum_{F\in\mathcal{F}_h} \|J_{h,1}\boldsymbol{v} - \boldsymbol{v}\|_{L^2(F)}^2 + \|J_{h,2}\boldsymbol{\sigma} n_F - \boldsymbol{\sigma} n_F\|_{L^2(F)}^2\Big)^{1/2} |y_h|_{s_h^p}\\
&\lesssim h^{k+1/2}\Big(\sum_{K\in\mathcal{T}_h} |x|_{H^{k+1}(K)}^2\Big)^{1/2} |y_h|_{s_h^p},
\end{aligned}$$

where we used the approximation properties (A.7) in the last estimate. A similar estimate shows that

$$|\langle S_h^p(J_h x - x), y_h\rangle_{L^2}| \lesssim h^{k+1/2}\Big(\sum_{K\in\mathcal{T}_h} |x|_{H^{k+1}(K)}^2\Big)^{1/2} |y_h|_{s_h^p},$$

which proves the claim since $S_h = S_h^s + S_h^p$. □

Institute for Applied and Numerical Mathematics, Karlsruhe Institute of Technology, Englerstrasse 2, 76149 Karlsruhe, Germany

Email address: benjamin.doerich@kit.edu

Institute for Applied and Numerical Mathematics, Karlsruhe Institute of Technology, Englerstrasse 2, 76149 Karlsruhe, Germany

Email address: julian.doerner@kit.edu